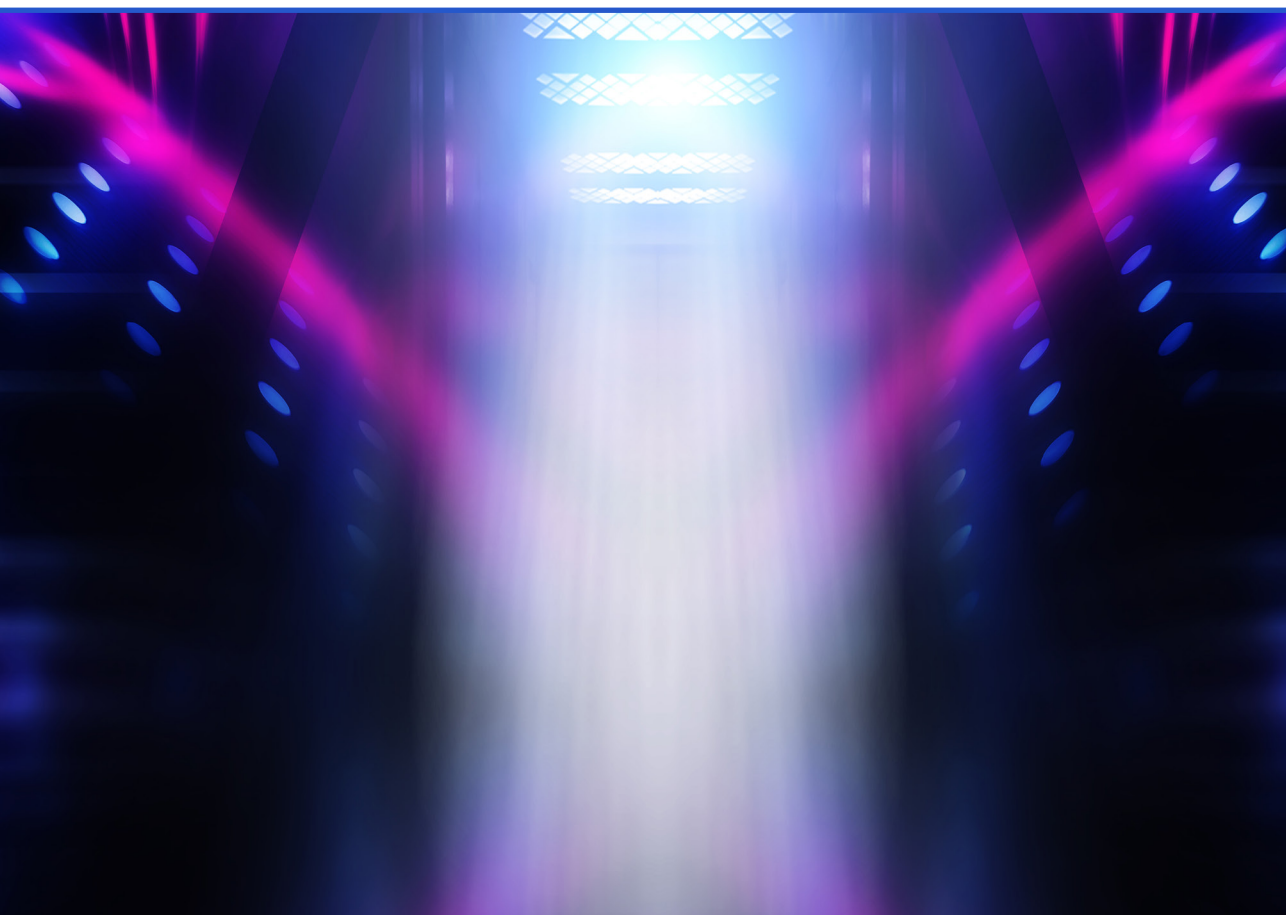


Aleksandrs Nevskis

**DYNAMIC PROPERTIES OF THE AIRCRAFT'S
FULL-SCALE COMPONENT TEST SETUP AND ITS
VIBRATION-BASED SYSTEM OF STRUCTURAL
HEALTH ASSESSMENT**

Doctoral Thesis



RIGA TECHNICAL UNIVERSITY
Faculty of Mechanical Engineering, Transport and Aeronautics
Institute of Aeronautics

ALEKSANDRS NEVSKIS
Doctoral Student of the Study Programme «Transport»

**DYNAMIC PROPERTIES OF THE AIRCRAFT'S FULL-
SCALE COMPONENT TEST SETUP AND ITS
VIBRATION-BASED SYSTEM OF STRUCTURAL
HEALTH ASSESSMENT**

Doctoral Thesis

Scientific Advisor
Prof. Dr. habil. sc. ing.
VITĀLIJS PAVELKO

Scientific consultant
Prof. Dr. habil. sc. ing.
MĀRTIŅŠ KLEINHOFS

Riga 2023

ANOTĀCIJA

Promocijas darba satur: anotācija (latviešu, angļu un krievu valodā), 9 nodaļas, 91 lapa, 71 attēls, 7 tabulas, 47 atsauces uz autoritātēm.

Atslēgas vārdi: testa iestatīšanas dinamiskā izturība, konstrukcijas datoru simulācija, modālā analīze, uz vibrāciju balstīts NDT, bojājumu indekss, konstrukcijas tehniskā stāvokļa uzraudzības sistēma

Promocijas darbs ir vērsts uz gaisa kuģa pilna mēroga komponentu un testēšanas aprīkojuma dinamisko īpašību novērtēšanas, dinamiskās izturības un konstrukcijas tehniskā stāvokļa uzraudzības problēmām dažāda veida stenda testa laikā.

Tiek sniegts apskats par gaisa kuģu struktūras testēšanas problēmām vēsturiskajā, tehniskajā un tehnoloģiskajā aspektā.

Pirmkārt, tika ņemtas vērā sarežģītas dinamiskās sistēmas pamatīpašības, tās strukturālo komponentu mijiedarbība, robeža nosacījumu ietekme, kā arī adekvāts sistēmas "lidaparāts - testēšanas ierīce" apraksts. Vienkāršam struktūras modelim un vispārējā tipa elastīgajai sistēmai tika pievērsta uzmanība. Šis izpētes mērķis ir uzlabot testa aprīkojuma parametru projektēšanas un optimizācijas metodes, ņemot vērā dinamiskās izturības prasības.

Tika parādīts, ka katrai liela mēroga struktūras modai ir atbilstoša frekvenču josla, kur augstākas modas modālās frekvences un modālās formas ir visjutīgākās pret vietējiem maza mēroga bojājumiem. Tiek piedāvāta efektīva aptuvena lokālo bojājumu simulācijas metode, lokāla vienas brīvības pakāpes oscilatora veidā.

Cits galvenais pētījumu virziens ir vērsts uz testa kompleksa tehniskā stāvokļa uzraudzības sistēmas uzlabošanu, jo īpaši uz vibrāciju nesagraujošās testēšanas metodes izmantošanu. Tas ir saistīts ar šīs metodes relatīvo vienkāršību un uzticamību, tās dabisko pielāgošanās spēju pastāvīgi kontrolēt dinamiski izkrautu struktūru normālas darbības laikā.

Tiek analizēts novatorisks analītisks risinājums relatīvi nelielu strukturālu bojājumu noteikšanai, izmantojot darbības ierosmi (OMA pieejas ietvaros). Vienkāršotās skaitļošanas simulācijas pieejas, ko plaši izmanto, lai novērtētu dažāda veida bojājumu ietekmi uz elastīgās struktūras dinamisko reakciju (plaisa, robežnosacījumu mainība, skrūvju savienojumu atslābināšanās). Eksperimentālās izmeklēšanas laikā izmantotā pseido bojājumu tehnoloģija.

Tiek piedāvāts daudzsoļš bojājumu indekss nelielu strukturālu bojājumu noteikšanai lielā mēroga konstrukcijas elementā, izmantojot struktūras dinamiskās frekvences reakcijas korelāciju. Tika iegūti testa dati īpašā dinamiskā testā ar pilnas skalas struktūru (helikoptera astes bumu) harmoniskā ierosmē un izmantoti, lai analizētu uz vibrācijām balstītas bojājumu noteikšanas metodes efektivitāti. Līdzīgs tests ar āmura trieciena ierosmi tika veikts arī ar otru pilna mēroga strukturālo komponentu

Tika veikts izstrādātā modeļa precizitātes un ticamības statistiskais novērtējums, kā arī strukturālo bojājumu noteikšanas varbūtības novērtējums.

Tiek dots testa stenda izstrādes piemērs ar tā dinamiskās izturības analīzi un iebūvēta nepārtrauktas stenda un testa objekta tehniskā stāvokļa uzraudzības elementiem.

ANNOTATION

The doctoral Theses consists of: annotation (Latvian, English and Russian), 9 chapters, 91 pages, 71 figures, 7 tables, 47 references to authorities.

Key words: dynamic strength of test setup, computational simulation, modal analysis, vibration-based NDT, damage index

The Doctoral Thesis is focused to the problems of dynamic properties estimation, dynamic strength and structural health monitoring of the aircraft full-scale component and testing equipment during of different types stand test.

There is given review of the problems of aircraft structure ground testing in historical, technical and technological aspects.

First, the fundamental features of complex dynamic system, interaction of its structural components, effect of boundary conditions and also adequate description of system 'test setup-aircraft component' were considered for some simple model of structure and the elastic system of general type. This investigation is aimed of improvement of designing and optimizing methods of parameters of test equipment taking in account the requirements of dynamic strength.

There was showed that for each mode of large scale structure there is corresponding frequencies band where the modal frequencies and modal shapes of higher modes are the most sensitive to local small-scale damage. The effective approximate method of local damage simulation in the kind of local, one degree of freedom oscillator is proposed.

Another main direction of research focuses on improving the system for monitoring the technical condition of the test complex, in particular, on the use of vibration non-destructive testing. This is due to the relative simplicity and reliability of the method, its natural adaptability for continuous monitoring of a dynamically unloaded structure in the course of its normal functioning.

An innovative analytical solution for the detection of relatively small structural damage using operational excitation (within the OMA approach) is analyzed. The simplified approaches of computational simulation widely used for estimation of the effect of different kinds of damages to dynamic response of elastic structure (crack, boundary condition varying, bolt-joints loosening). The pseudo-damage technology used during experimental investigation.

A promising damage index is proposed for detecting small structural damage in a large structural element using the correlation of the dynamic frequency response of the structure. Test data in special dynamic test on the full-scale structure (tail boom of helicopter) at harmonic excitation was obtained and used in analysis of efficiency of vibration-based method of damage detection. Similar test with hammer-blow excitation was done on the other full-scale structural component

A statistical assessment of the accuracy and reliability of the developed model was carried out, as well as an assessment of the probability of detecting structural damage.

An example of the development of a test bench with an analysis of its dynamic strength and elements of built-in continuous monitoring of the technical state of the bench and the test object is given.

АННОТАЦИЯ

Докторская диссертация состоит из: аннотации (на латышском, английском и русском языках), 9 глав, 91 страницы, 71 рисунка, 7 таблиц, 47 ссылок на авторитетные источники.

Ключевые слова: динамическая прочность испытательной установки, компьютерное моделирование, модальный анализ, неразрушающий контроль на основе вибрации, индекс повреждений, мониторинг состояния конструкций.

Докторская диссертация посвящена проблемам оценки динамических свойств, динамической прочности и контроля состояния конструкции натуральных компонентов и испытательного оборудования самолета во время стендовых испытаний различных типов.

Дан обзор проблем наземных испытаний конструкции самолета в историческом, техническом и технологическом аспектах.

Сначала были рассмотрены фундаментальные особенности сложной динамической системы, взаимодействие ее структурных компонентов, влияние граничных условий, а также адекватное описание системы «испытательная установка - элемент самолета» для некоторой простой модели конструкции и упругой системы общего типа. Исследование направлено на совершенствование методов проектирования и оптимизацию параметров испытательного оборудования с учетом требований динамической прочности.

Было показано, что для каждой моды крупномасштабной структуры существует соответствующая полоса частот, где модальные частоты и модальные формы более высоких мод наиболее чувствительны к локальным мелкомасштабным повреждениям.

Проанализировано инновационное аналитическое решение для обнаружения относительно небольших структурных повреждений с использованием оперативного возбуждения (в рамках подхода ОМА). Упрощенные подходы компьютерного моделирования широко используются для оценки влияния разного рода повреждений на динамическую реакцию упругой конструкции (трещина, изменение граничных условий, ослабление болтовых соединений). Технология псевдо-повреждений, использована при проведении экспериментальных исследований на натурной конструкции.

Предлагается перспективный индекс повреждения для обнаружения небольших структурных повреждений в крупном структурном элементе с использованием корреляции динамических реакций поврежденной и базовой (неповрежденной) конструкций. Получены данные в специальных динамических испытаниях натурной конструкции (хвостовой балки вертолета) при гармоническом возбуждении, которые использованы при анализе эффективности вибрационного метода обнаружения повреждений. Аналогичное испытание с возбуждением ударом молотка было проведено на другом полномасштабном структурном элементе.

Проведена статистическая оценка точности и надежности разработанной модели, а также оценка вероятности обнаружения повреждений конструкции.

Приведен пример разработки испытательного стенда с анализом его динамической прочности и элементами встроенного непрерывного мониторинга технического состояния стенда и объекта испытаний.

Contents

1. Introduction. The aim and main problems of research.....	7
2. Review of the aviation equipment strength testing issue.....	9
2.1. Strength testing of aircraft structures and their classification	11
2.1.1. Static strength testing.....	12
2.1.2. Fatigue strength testing	12
2.1.3. Periodic manufacturing quality control.....	13
2.1.4. "Survivability" testing.....	13
2.1.5. Laboratory testing of material samples	16
2.2. Equipment for full-scale strength tests, control and measurement systems.....	16
2.2.1. Facilities for static strength testing	16
2.2.2. Facilities for breaking testing.....	23
2.2.3. Facilities for laboratory testing of material samples	29
2.3. Description of structural strength defects and assessment of their impact on strength	30
2.4. Methods and technologies for detecting structural strength defects, equipment	33
3. Analytical study and computer-aided simulation of dynamic properties of aircraft component in full-scale test.....	34
3.1. On the Properties of Solutions of the Structural Dynamics of Elastic Systems	34
3.2. Simple Example: A Cantilever Beam With an Elastic Clamping	34
3.3. Dynamic Properties and Response of the Structure	35
4. Vibration-based detection of structural damage in full-scale test	37
4.1. Fundamentals of method (dynamic properties, dynamic response to different types of excitation, EMA and OMA approaches of dynamic properties evaluation and damage detection, board band excitation and frequency response function, transience function).....	37
4.2. General problems of vibration based method (VBM) application	37
4.3. The basic idea of innovative approach of a damage detection by VBM: the use of group evolution of higher modes.....	38
5. Experimental study and method validation	40
5.1. Full-scale comp used in the test	40
5.1.1. Study on the tail boom of the Mi-8 helicopter	40
5.1.2. Study on the tail boom of the Ka-62 helicopter.....	41
5.2. The objective of test and equipment	44
5.2.1. The objectives of test	44
5.2.2. Test setup	44

5.3. Test results	45
5.4. Discussion and feature extraction.....	46
6. Statistical Estimation of Perspective Damage Index for Vibration-Based Structural Health Monitoring ...	48
6.1. About Test Setup and Measurement Equipment	48
6.2. Some Important Results of Research.....	48
6.3. Data Acquisition and Statistical Analysis.....	49
7. An example of the test facility development with an analysis of its dynamic strength and elements of built-in continuous monitoring of the technical state of the test facility and object	53
7.1. Main priorities and stages of test facility creation.....	53
7.2. Facility creation purpose.....	53
7.3. Purpose of the main parts of the facility	54
7.4. Technical requirements for facility design	55
7.4.1. Helicopter.....	55
7.4.2. Power frame	55
7.5. Calculation of the facility strength and dynamic parameters	56
7.5.1. Work purpose, initial information features and problem-solving method	56
7.5.2. Generalized results of strength assessment of the main facility structure without OS	63
7.5.3. Strength calculation of the main facility structure with installed object simulator	67
7.5.4. Analysis of loading and strength of supports	70
7.5.5. Modal analysis of dynamic features of the facility.....	75
7.6. Receiving signals from the Facility Measurement System and their processing	77
7.6.1. Type of applied accelerometers	78
7.6.2. Signal format received from the accelerometer.....	79
7.6.3. Examples of recorded accelerometer signals from the helicopter testing	80
8. Conclusions	86
9. Bibliography	88

1. Introduction. The aim and main problems of research

Relevance. To ensure the reliability of the operation of aviation equipment, the regulatory documents provide for a large range of activities, the purpose of which is to prove that the design meets the requirements. A key link in ensuring reliability is the testing of full-size structures or individual, most critical components thereof. The procedure for such tests is extremely expensive and, as a rule, takes considerable time. Therefore, improving the methods of planning, organizing and conducting tests, collecting and processing information, solving problems of control and test automation represent a range of topical scientific and technical problems, on the basis of which the effectiveness of the tests and the reliability of their results depend. Some of these problems determine the motivation of this study.

The aim of Doctoral Thesis: Investigation of the dynamic properties of test complex of aircraft full-scale structural component and analysis of some version of the vibration-based system of structural health monitoring (SHM) .

The main problems of research:

1. Investigation of some general effects of the boundary conditions and their adequate description at the structural dynamic analysis.
2. Consideration of a simplified model of the elastically supported beam to evaluate the effects of the support compliance to the basic dynamic characteristics.
3. More complex modeling of the body elastic attachment
4. General problem of vibration-based method of NDT application for SHM in the full-scale test of aircraft components
5. Development of some solution for a relatively small structural damage detection using operational excitation (in the frame of the OMA approach).
6. Development of perspective appropriate damage index for detection small structural damage in the large structural component
7. Estimation of accuracy and reliability of developed VBM

Scientific novelty and areas of application

1. Some general properties of the boundary conditions and their adequate description at the structural dynamic analysis.
2. A simplified model of the elastically supported beam for evaluation of the effect of elastic constrains to the basic dynamic characteristics.
3. More complex general model of the body elastic attachment
4. General problem of vibration-based method of NDT application for SHM in the full-scale test of aircraft components
5. Innovative analytical solution for a relatively small structural damage detection using operational excitation (in the frame of the OMA approach).

6. Perspective damage index for detection small structural damage in the large structural component using correlation of a structure dynamic frequency response
7. Statistical estimation of accuracy and reliability of developed VBM, and evaluation of probability of the structural damage detection
8. The results of the doctoral thesis shall be oriented towards practical use in dynamic trials of aviation techniques.
9. The variant developed by the vibration-based design condition monitoring system can be interesting both for monitoring aviation designs and other industry structures and for their operation

2. Review of the aviation equipment strength testing issue

From the dawn of aviation, there was a natural understanding of the necessity to ensure a sufficient level of aircraft strength. Many attempts to take to the air at that time ended in accidents and disasters, and the ratio of destructions due to the structure's inability to withstand flight loads was very high. On the one hand, this situation was due to insufficient knowledge about flight loads in normal flight and the inaccuracy of their theoretical assessment. On the other hand, the assessment of the structure's bearing capacity was based on calculation methods developed in relation to the problems of other branches of technology and construction and were far from perfect at that time. These problems initiated the rapid progress of aviation science, the achievements of which were widely introduced into practice. Such a situation clearly illustrates an example of a change in the concept of the ultimate design load to be withstand by an aircraft. The design overload was taken as a measure of the ultimate design load applicable for a wide class of aircraft, which limited the limiting value of the structure's external load, which it should be able to withstand without destruction. The design overload value was established mainly on the basis of experience analysis. The design overload was refined within accumulation of the experimental data. In France, in 1911, the design overload value was set equal to 3, and the next year it was revised upwards to 3.5, and with the outbreak of World War in 1914, it was adopted as 4.5 [1]. The same situation was in Germany and Russia. When it comes to assessing the structure's bearing capacity, the aircraft manufacturers quickly came to understand a radical way to test it: full-scale tests of a full-scale structure or its most critical components.

Destructions of machines had place, because the first aircraft engineers did not know how to calculate the structure, what safety factors to take, and could not determine features of the materials used.

The first static tests of aircraft assemblies took place at the beginning of the 20s of the last century. During testing, the structure was loaded with the concentrated forces or a ballast loading method was used, when the loading was carried out with a load distributed over the surface using sand or shot bags. An example of such tests is shown in the Figure below.



2.1.0. Figure. Testing of the I-11 aircraft at the VEF factory (Latvia, 30s of the 20th century [54])

In the 1930s, the ballast method was replaced by loading with a lever system. With this method, the distributed load acting on the structure is replaced by small concentrated forces, which are reduced to one or more resultant forces by means of the system of levers and rods. The load is created by special power exciters, the number of which is equal to the number of resultants. This technique has significantly improved the loading accuracy. The design has become more open for visual observation and installation of measuring devices on the product surface. Now it is possible to instantly terminate the load and quickly remove it when the destruction is detected.

By the beginning of the 1940s, static tests had acquired decisive importance in assessing the strength of aircraft structures. The main result during this period was to determine the structure's actual strength by loading it to the design or even to the breaking load. Measurements of deformations with the subsequent determination of the deformed and stressed state of the structure are beginning to spread increasingly more.

In the late 1940s, application of wire strain gauges for static tests was started, which made it possible to organize mass tensometry of the main aircraft units and significantly expand the possibilities of studying and analyzing the actual stress state of the structure.

Today, the test complexes allow practically reproducing any given load affecting the aircraft. Modern measuring systems allow to receive information about the state of the test object with high accuracy.

Creation of the International Civil Aviation Organization (**ICAO**) had a great influence on the aircraft development. This organization has adopted the Standards and Recommended Practices on a number of issues affecting flight safety. In particular, the aircraft design and testing standards have been introduced, and the concept of the **aircraft airworthiness standards** has been defined.

The International Civil Aviation Organization (ICAO) has established that ICAO member countries should issue to their registered aircraft operated on the international flights a certificate that guarantees compliance with the Aircraft Airworthiness Standards (AAS) and a specified safety level. This rule was subsequently extended to aircraft operated within a single country. Each newly created civil aircraft should receive the airworthiness certificate. This certificate allows operation of an aircraft.

The Aircraft Airworthiness Standards and Recommended Practices were adopted by the Council on March 1, 1949 in accordance with the provisions of Article 37 of the Convention on International Civil Aviation (Chicago, 1944) and are designated as Annex 8 to the Convention.

It was recognized that the ICAO Aircraft Airworthiness Standards would not replace national regulations and that the national aircraft airworthiness codes, containing the full scope and level of detail deemed necessary by the individual states would be needed as a basis for certification of individual aircraft.

It also retains the requirement that each Contracting State should either establish its own comprehensive and detailed aircraft airworthiness code or select a comprehensive and detailed code established by another Contracting State.

The Council endorsed the above approach on March 15, 1972, which formed the basis of the current ICAO aircraft airworthiness policy.

Aircraft certification is assessment of the aircraft compliance with the AAS. At the same time, the aircraft airworthiness is controlled during the entire operation period of each aircraft. Experience shows that civil aircraft certification is a powerful tool for achieving safety.

To ensure the aircraft certification, it is necessary to determine the following by the beginning of its design:

- AAS applicable to the aircraft type and compliance determination methods;
- certification system that includes the rules for monitoring compliance and identifies the organizations responsible for certification;
- work program to ensure the aircraft's compliance with the AAS and certification. The program should include the necessary research, the creation of models, Facilities, modeling, bench and flight tests, as well as evidentiary documentation.

Comparative assessment of the AAS of the countries with the most developed aviation industries (USA, Russia, England and France) indicates that they determine almost the same level of civil aircraft airworthiness. The most respected are the US (FAR) and European (JAR) airworthiness standards, as well as Russian aviation regulations (AR).

2.1. Strength testing of aircraft structures and their classification

An important part of the aircraft creation works is strength provision. The main goal of these works is to prevent destruction or irreversible changes and to limit the relative deformations (within certain limits) of structural elements under the effect of loads arising from the aircraft operation. At the same time, the aircraft should maintain the range of features specified by the technical requirements during design.

The path of increasing the cross-sectional areas of structural elements to ensure strength leads to a decrease in the aircraft flight efficiency, which is unacceptable. The problem of finding an optimal solution that provides strength with a minimum weight is solved.

To successfully solve this problem, it is necessary to understand well what loads act on the aircraft, affecting the strength features, to master the methods of theoretical and experimental study of the aircraft elements for strength.

The types of strength tests of aircraft structures are a consequence of the type of loads affecting the aircraft during its operation.

In fact, strength tests are a criterion of truth for designers.

Such tests are an opportunity to identify weak points in a design that need to be modified or replaced.

2.1.1. Static strength testing

The loads experienced by the aircraft during its operation can be divided into two types: static loads and dynamic loads.

Static load - constant or slowly changing over time. The time of its application to the structure is much longer than one period of natural oscillations of the fundamental tone of the apparatus structure. In this case, the load increases monotonically. If this load exceeds a certain value, then destruction will occur. An increase in the load above a certain value entails irreversible changes (permanent deformations). Residual deformations do not disappear after the load removal. In this case, one loading cycle is sufficient. The loads at which destruction occurs are called estimated P_p . The magnitude of these loads should be greater than the loads arising during the aircraft operation. The maximum loads arising during the aircraft operation are called operational P_e . The P_p value should be greater than the P_e value

$$P_p > P_e \text{ (2.1.1)}$$

When designing, they are guided by the expression following from (2.1.1), specified in voltages

$$\sigma_p > \sigma_e \text{ (2.1.2)}$$

Experimental verification of inequality (2.1.2) is mandatory and is carried out using brassboards especially designed for a specific object. This type of test is called **static strength test**.

2.1.2. Fatigue strength testing

Damaging consequences can arise from loads of lesser magnitude, if they repeatedly affect the structure. Structure may be destructed after exposure to not one, but a certain number of loading cycles (the so-called fatigue loading). Such loads are called dynamic. Dynamic load (shock or vibration) has a number of parameters. One of them is distinctive - the time of its application to the structure is commensurate with the period of oscillations of the fundamental tone. The structure is elastic and will perform elastic vibrations under the influence of time-varying external loads. These vibrations will cause additional dynamic loads on the structure. The presence of load variable component inevitably leads to the appearance of time-varying deformations of structural elements and, as a consequence, to variable stresses in them. Therefore designers are often guided by the following conditional inequality

$$\sigma_{e.p} < \sigma_{w.g.} \text{ (2.1.3)}$$

where $\sigma_{e.p}$ - stresses acting in flight (determined by calculation);

$\sigma_{w.g.}$ - guaranteed endurance limit (values of alternating stresses known from experience, at which the resource of structural elements will be large enough).

Inequality (2.1.3) is intermediate, meaning only in design. The final criterion is resource value, which is determined by the calculation and experimental method for the finished product using a special brassboard. Tests of this type are called **fatigue tests**.

Strength calculations are carried out taking into account the action of static and dynamic loads. The combination of the required values of various types of strength (static and fatigue) that ensure the structure's normal operation within the established limits and terms is called **operational strength**.

During operation, the structure's strength does not remain constant. Heavy loads can cause permanent deformations in the structure. Small but repetitive loads cause the development of fatigue cracks weakening the structure.

2.1.3. Periodic manufacturing quality control

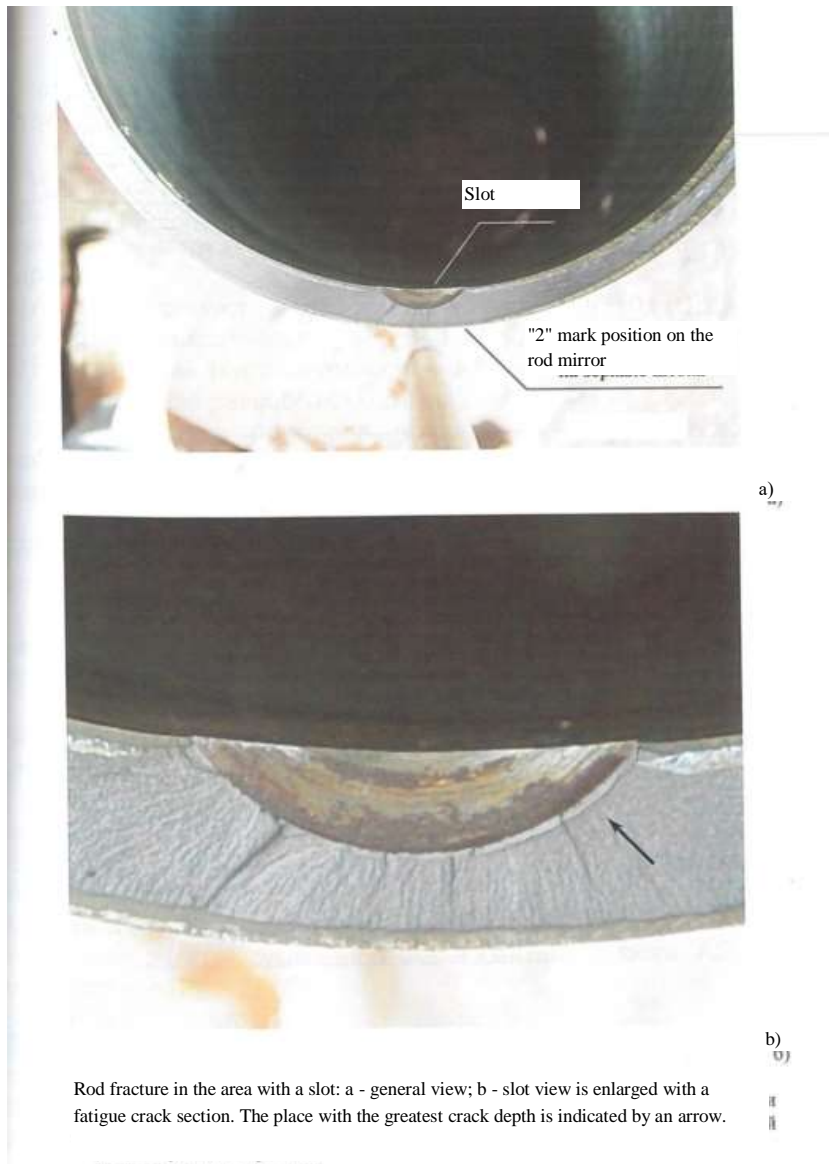
In serial production, the main task of ensuring strength is to control the quality of serial products. The main means of solving this problem is systematic testing of samples of serial products at the Facilities. Such tests are called **periodic**. The number of samples sent for periodic testing is determined according to special methods, taking into account the design features and criticality in the overall supporting system. In this case, tests can be made both for static and fatigue strength.

2.1.4. "Survivability" testing

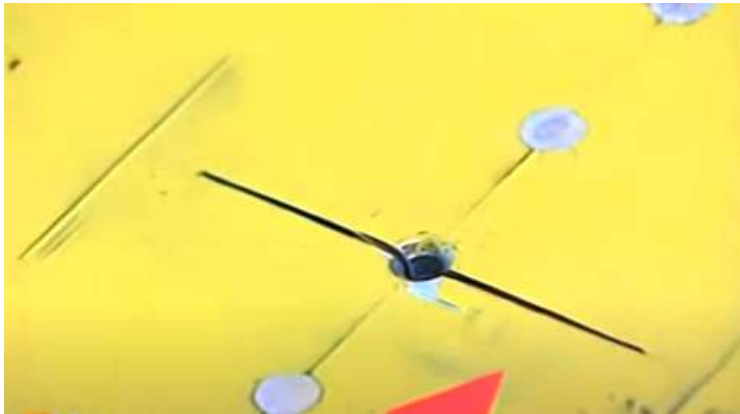
"Survivability" tests are carried out for a more complete study of the aircraft structure. "Structure's survivability" shall mean its ability to maintain its overall bearing capacity in case of local destructions. In this case, "destruction" is introduced in the investigated structural element, usually in the form of an artificial crack or violation of the structure's regularity. Then a cycle of dynamic tests is carried out at a facility.

This method is illustrated in Figures 2.1.1-2.1.2.

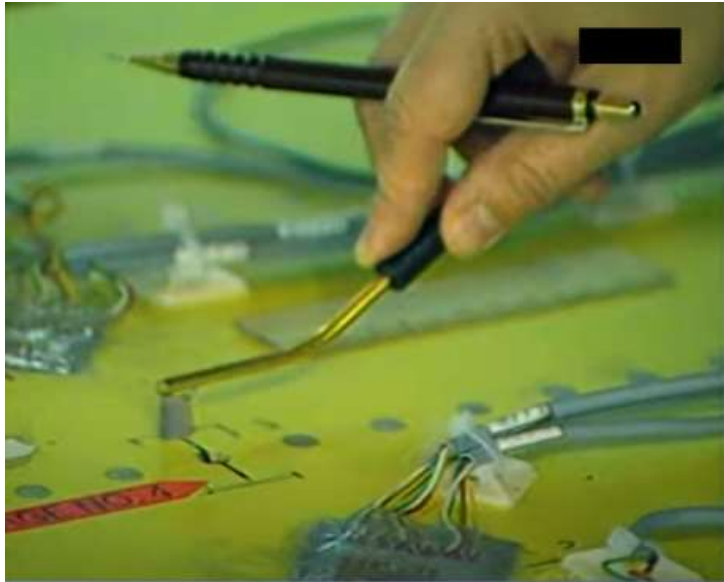
«Destruction» (an artificial crack) is introduced into the aircraft's landing gear rod:



2.1.1. Figure. Illustration of the "survivability" test method for the aircraft landing gear rod «Destruction» (an artificial crack) is introduced into casing of the aircraft torsional box



a)



b)

2.1.2. Figure. Illustration of the "survivability" test method for an aircraft wing [48]

2.1.2 a) Imitation of a crack in a structure

2.1.2 b) Control of crack growth during loading

These studies allow us to conclude that the object can be operated in the presence of a crack.

2.1.5. Laboratory testing of material samples

Hooke's Law describes basic mechanics of elastic bodies. However, the use of this law was impossible without establishing the physical constants of materials binding the force value with elastic deformation. The constants themselves are the coefficient of elasticity and the transverse deformation ratio.

It is impossible to calculate the strength, rigidity and stability of any structure without first experimentally determining the longitudinal elasticity modulus

E (Young's modulus), shear modulus (G) and Poisson's ratio
(ν) for the structure's material.

In addition, without preliminary experimental determination of the maximum stresses that a material can withstand under tension, torsion, shear, it is impossible to formulate a strength condition and select the structure's permissible load or safe dimensions.

Such experimental studies of material properties are carried out in the specialized laboratories for testing materials that exist at the design bureaus of factories, research and educational organizations.

The tests are carried out on samples made of metal and composite materials.

Test types: tensile, compression, shear, hardness, impact strength

Examples of Facilities illustrating the test types are shown in the next section.

2.2. Equipment for full-scale strength tests, control and measurement systems

It is difficult to describe the variety of Facilities designed in the global aviation industry in one paper. This chapter shows examples of test Facilities that characterize the main types of aircraft testing.

2.2.1. Facilities for static strength testing

2.2.1.1. Facilities for static strength testing of full-scale aircraft

Figures 2.2.2, 2.2.3, 2.2.4 show examples of objects when tested for static strength. The object represents a full-size aircraft fuselage. Through the simulators, the chassis is fixed to the power floor. Engines are also being replaced by imitators. In the passenger compartment, the appropriate load is distributed to simulate the weight. Loading is carried out using hydraulic cylinders, which are attached to the power frame. The power frame is part of the stand. The power frame is important for loading, the loading accuracy depends on it. Usually the power frame has a safety margin of at least 3. The force in the hydraulic cylinders is controlled by a central computer with great accuracy. Places of application of force simulate the load in real flight. When testing for static strength, as a rule, loading is carried out to a level of loads equal to the operational ones. Next, load is carried out to the calculated level. Design loads are often destructive.



2.2.2. Figure. Facility for full-scale static tests of A-380 aircraft [51]



2.2.3. Figure. Facility for full-scale static tests of A-350 aircraft [51]



2.2.4. Figure. Facility for full-scale static tests of an aircraft [51]

When testing the static strength of a full-size helicopter fuselage, similar stands are designed. Helicopter static strength tests are more complex. When loading, the fuselage must be “balanced by loads.” For this, special schemes are being developed to balance the fuselage. Loading is also carried out using hydraulic cylinders. For example, Figure 2.2.5 shows a stand for testing a helicopter fuselage for static strength.



2.2.5. Figure. Facility for full-scale static tests of a helicopter [55]

2.2.1.2. Facilities for static tests of aircraft components

Static tests are also carried out for individual aircraft and helicopter components. In this case, the correct fixing of the object to the stand is of fundamental importance. The place of attachment should imitate the attachment of the object to the fuselage as accurately as possible and have a sufficient margin of safety. This is achieved by preliminary calculation of the strength of the test equipment. As well as for a full-sized fuselage, it is important to apply design loads to the object. They can be "point" and "distributed". As a rule, tests are carried out for operational loads and design loads. Figures 2.2.6 - 2.2.10 show examples of benches for testing individual units.

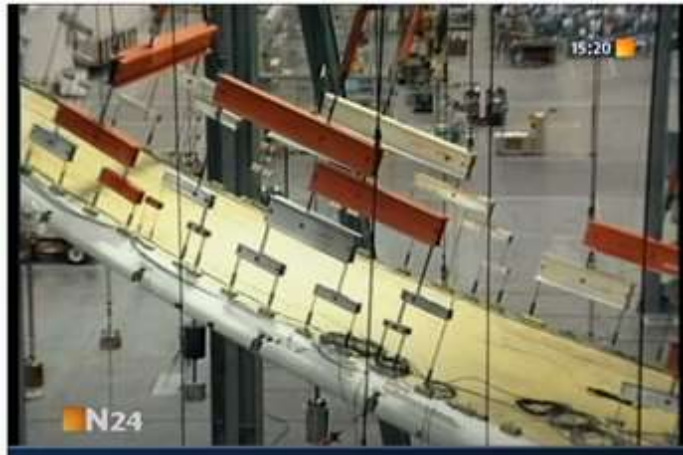


a) General form



b) Flap attachment compartment

2.2.6. Figure. Facility for static tests of A-380 aircraft wing torsion box [49]



a) Structure loading



b) Destruction

2.2.7. Figure. Destruction test of a structure's component [48]

On this stand, the load on the object is applied to the “calculated” level. As a result, the object may be destroyed.



a)



b)

2.2.8. Figure. Testing of wing torsion box a) and engine mounts b) of A-380 aircraft [48]

Tests of individual nodes are often carried out together in one unit. It is logical to test the wing box and the engine mount.



2.2.9. Figure. Testing of the aircraft passenger cabin floor [51]

In this case, the floor of the passenger cabin is tested. To distribute the load, a system of special lodgements is used.



2.2.10. Figure. Airframe wing static test [53]

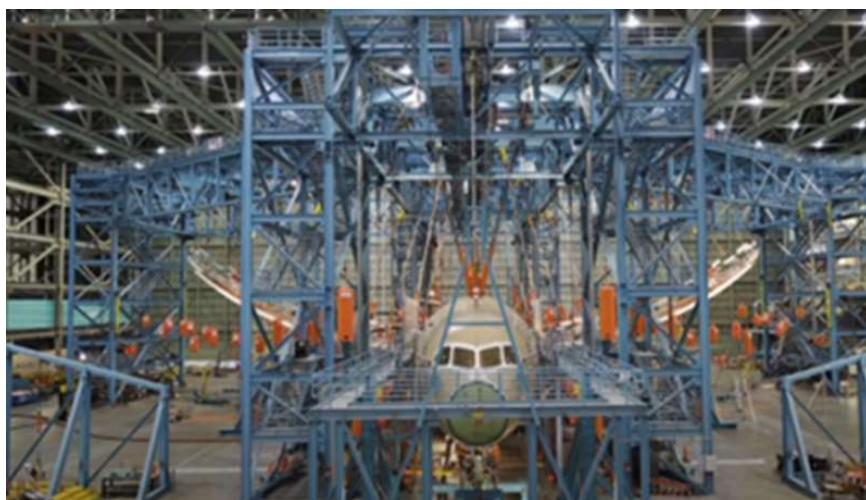
To set the load when testing the glider wing, a system of lodgements was used. Each lodgment is located along the power rib. A feature of the airframe wing test is its high bending flexibility (compliance).

2.2.2. Facilities for breaking testing

When testing for fatigue, stands are designed taking into account the fact that a load that is repeated in time is applied to the test object. The test object is attached to the power frame or power floor. The object is loaded using hydraulic cylinders. Sometimes the method of loading through a kinematic mechanism using an electric motor is used. As a rule, tests are carried out for operational loads.

2.2.2.1. Facilities for breaking testing of full-scale aircraft

Figure 2.2.11 shows the Boeing 787 Full-Scale Fatigue Test Bench. This bench implements a load application scheme that is as close as possible to a real flight. It is also possible to load individual parts of the fuselage and wing in accordance with the test program.

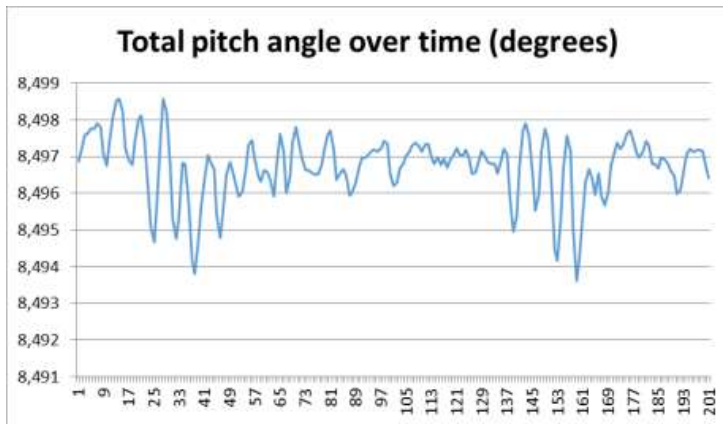


2.2.11. Figure. Facility for full-scale breaking testing of Boeing 787 aircraft [52]

There is a separate type of helicopter testing when it is necessary to test the main gear, tail gear, transmission and carrier system in operation. In this case, the helicopter is mounted on a specially designed power frame. The power frame must ensure the fixed position of the fuselage in all engine operating modes. The operation of the engines and the carrier system is controlled remotely from a special control center. From the carrier system of the helicopter and transmission, dynamic loads are transferred to the power frame. Therefore, special requirements are imposed on the strength of the stand. Destruction of parts of the stand is unacceptable. **Even slight changes in the rigidity of the bench elements can lead to a deviation of the specified loads on the test object.** The power frame with the fuselage installed on it is calculated for dynamic strength. Diagnostic systems are used to monitor the condition of the stand elements. An example of designing a similar stand is described in Chapter 7. Figure 2.2.12 –a) shows the stand for full-scale tests on the main gearbox, transmission and carrier system of the Mi-26 helicopter [56]. Figure 2.2.12 - b) shows an example of a “cyclogram” of a dynamic change in the angle of the main rotor blades. These dynamic angle changes are the main source of vibration in the bench.



a)



b)

2.2.12. Figure. Facility for full-scale breaking testing of the main gearbox, transmission and carrier system of Mi-26 helicopter [56]

a) general view of the test bench

b) example: dynamic change in the angle of rotating blades

The problem of monitoring the state of the structure is especially important for helicopters. As you know, there are especially many critical points in the design of a helicopter. There are examples of using the built-in monitoring system for the Agusta-Bell AB139 helicopter [68]. The system is based on load control in hazardous areas. If the value of a particular index reaches a dangerous level, the system gives a signal.

2.2.2.2. Facilities for breaking testing of aircraft elements

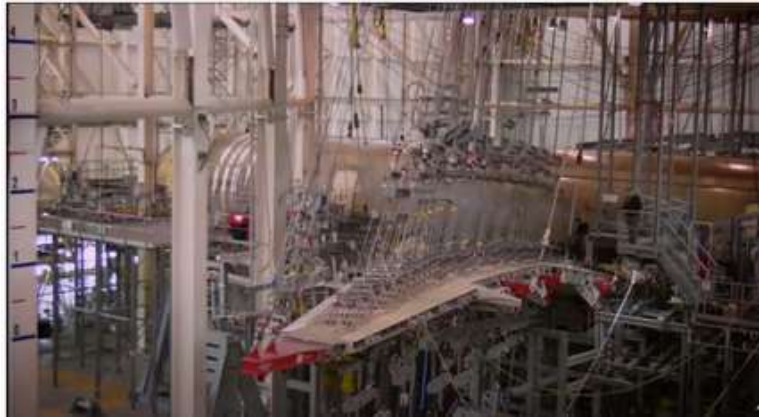
As well as for static tests, fatigue tests are carried out for individual components of the aircraft and helicopter. Figures 2.2.13 - 2.2.16 show examples of benches for testing individual units for fatigue.

Figures 2.2.13 - 2.2.14 show benches for testing the aircraft wing box for fatigue. With such a test, the aircraft fuselage is rigidly fixed to the power floor. The fuselage in this case is an element of the stand.

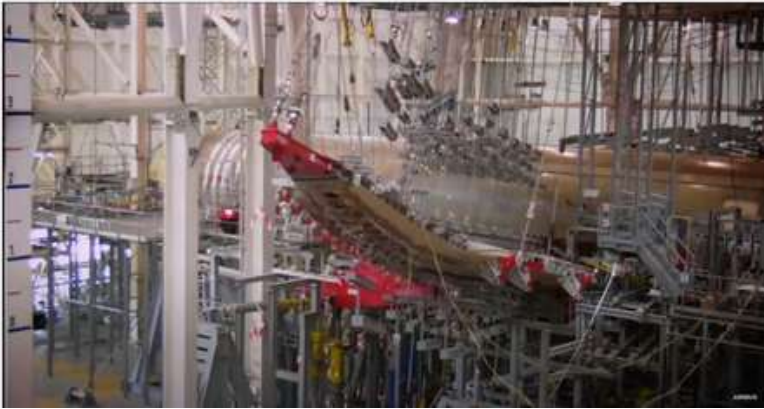


2.2.13. Figure. Facility for breaking testing of Boeing 787 aircraft wing [50]

A feature of loading the wing box on this stand is that the loads from the hydraulic cylinders are transmitted through special “lodgements”.



a)



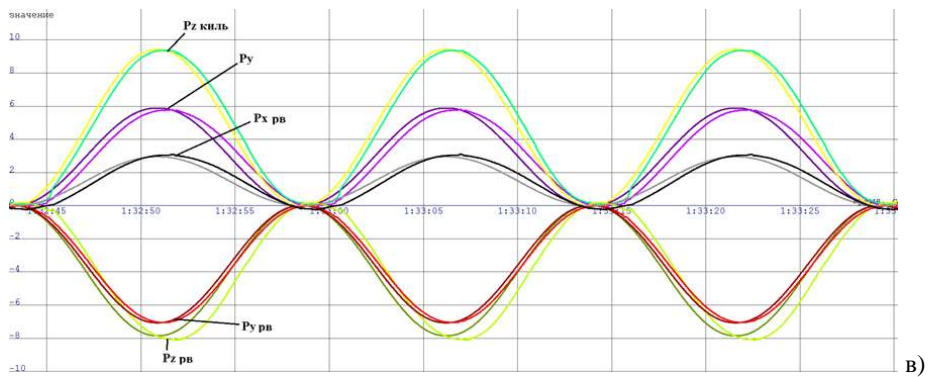
b)



c)

2.2.14. Figure. Breaking testing of A-350 aircraft wing: a), b) c) - loading process [49]

On this bench, the loads from the hydraulic cylinders are transferred to the wing box through a system of levers.



2.2.15. Figure. Facility for tail boom and helicopter fin testing [57]

Figure 2.2.15 a) shows a bench for testing the keel and tail boom of a helicopter for fatigue. With such a test, the helicopter fuselage is rigidly fixed to the power floor. The fuselage in this case is an element of the stand.

Figure 2.2.15 б) shows an example of a “cyclogram” of loading. In this example, 5 loading channels are used: in the keel and tail boom areas. Loading in the channels is carried out without phase shift.



2.2.16. Figure. Helicopter fenestron testing facility [58]

Figure 2.2.16 shows a bench for testing the helicopter fenestron for fatigue. With such a test, the fenestron of the helicopter is rigidly fixed to the power frame. The load is applied by a hydraulic cylinder along the axis of the fenestron.

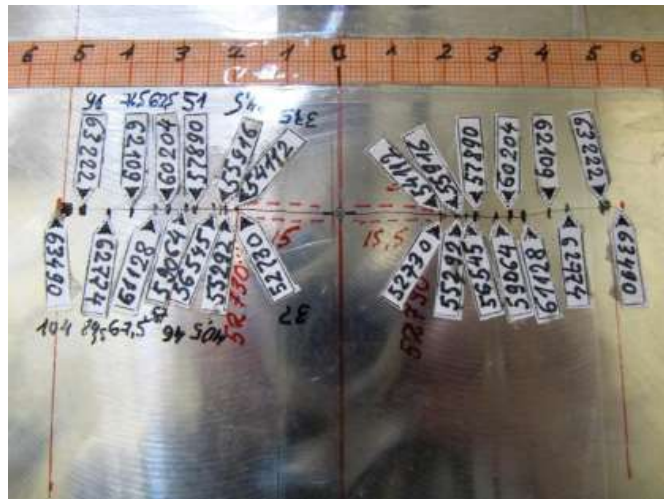
2.2.3. Facilities for laboratory testing of material samples

For strength testing of material specimens, hydraulically driven equipment is usually used. Such equipment today has a large range of loads and high accuracy of load control. This equipment allows you to apply a load to the sample both in static mode and in dynamics.

Figure 2.3.1 shows the test material sample, which is fixed on the testing machine.



2.3.1. Figure. Testing of samples material [59]



2.3.2. Figure. Control of crack growth in a sample. Numbers represents quantity of a sample loading cycles [59]

Figure 2.3.2 shows a sample of a material under fatigue testing. When a crack appears, its length is fixed. In this case, information on the number of loading cycles is installed on the sample.

2.3. Description of structural strength defects and assessment of their impact on strength

In the course of strength tests, the test object is examined to determine destruction and permanent deformations.

As indicated in the previous sections, there are static strength and breaking tests. During static tests, the studied object is loaded once and the structure is inspected once as well. In breaking tests, inspection is carried out many times after a certain number of loading cycles until the moment.

If the object is destroyed as a result of inspection, then the destruction analysis will be performed.

Fractures are cleaned after inspection. Fractures are inspected organoleptically and using the optical flaw detection methods. As a rule, inspection is carried out with gradual transition and increasing magnification.

Inspection helps to find the crack initiation place and determine its propagation rate.

Fractures are photographed under oblique illumination for the clearest transmission of the fracture's structural features in the photograph. Crystalline breaks are photographed in a shaded field to avoid glare. The magnification is selected so as not to reduce the image depth.

If there is a part with fatigue destruction among several destructed parts, it can be considered that it was destructed first.

Material destruction during strength tests can be divided into two main types, corresponding to two main types of tests: static strength and breaking.

Three main areas can be distinguished at the fracture area using breaking test:

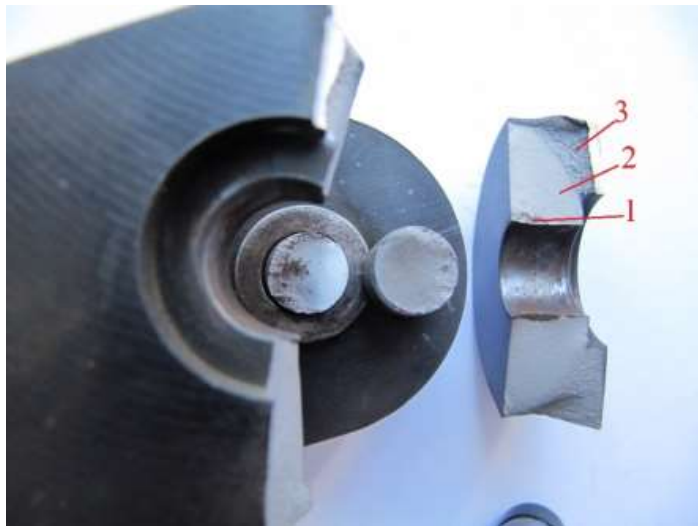
- crack initiation area;
- fatigue growth area. In this case, the crack has already appeared, but the object can withstand the load. When inspected, this area usually has a fine-grained structure;
- static rupture area. At the same time, the working section area has decreased to such an extent that the object cannot withstand the acting load, which is equivalent to static loading. When inspected, this area has a coarse-grained structure. An example of material fracture during breaking tests is shown in Figure 2.3.3.

When tested for static strength, the fracture usually has a uniform coarse-grained structure. An example of material failure during static strength tests is shown in Figure 2.3.4.

destruction of an object made of a composite material has a distinctive form associated with the delamination of layers and the destruction of fibers. Destruction of an object made of composite material is shown in Figure 2.3.5



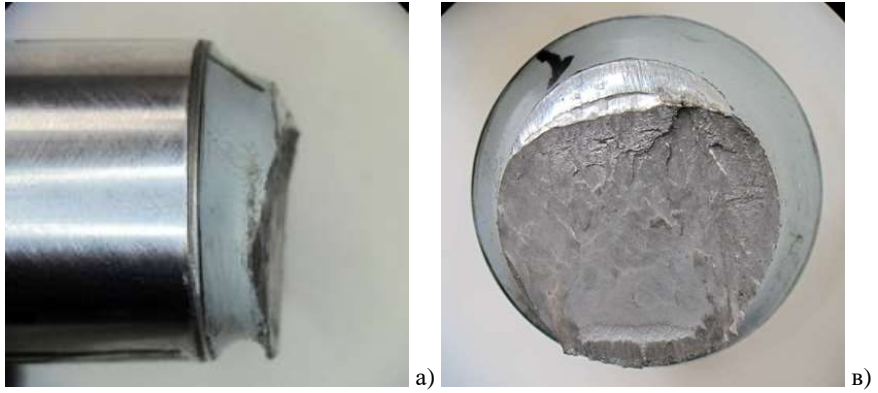
a) General view



a) Increased

- 1- crack initiation area
- 2 - fatigue growth area
- 3 - static rupture area.

2.3.3. Figure. Example of material destruction during breaking tests [60]



2.3.4. Figure. Example of material destruction during static strength tests [60]



2.3.5. Figure. Destruction of fuselage skin made of composite material [61]

2.4. Methods and technologies for detecting structural strength defects, equipment

With all the variety of defects arising in the aircraft structures, they are all united by a common feature: they cause a noticeable change in the physical features of the material - density, electrical conductivity, magnetic permeability, elastic properties, etc. In this case, defects, which are various violations of the structure's continuity, cause a sharper change in the material properties.

The study of changes in the physical features of the material and the detection of imperfections in its structure - defects, - constitutes the physical basis of non-destructive testing methods.

Non-destructive testing is used in the manufacture of aircraft structures, subsequent operation and during strength tests.

The energy of destruction dictates the need to create methods, the sensitivity of which can ensure the detection of emerging cracks at the very initial stage of their development. The crack propagation rate can be very high in parts made of high-strength materials subjected to complex loading. In order to prevent danger, it is necessary to improve methods that allow detecting the preliminary destruction areas.

Continuous improvement of the structure's state monitoring methods during testing of aircraft structures contributes to the improvement of the quality of tests and helps to reduce their cost.

Non-destructive testing makes it possible to assess the state of an object without dismantling and taking samples, which are quite expensive.

When testing aircraft structures, the non-destructive testing methods are used depending on the physical principles at their basis:

visual-optical control - this method is the simplest, the least time consuming and relatively inexpensive;

- **magnetic** - this method is based on the analysis of a magnetic field interaction with a controlled object;

- **electric** - this method is based on recording the parameters of an electric field interacting with a controlled object;

- **eddy current** - eddy current methods can be used during the inspection of electrically conductive products when detecting defects, structural inhomogeneities and deviations from the chemical composition. Eddy current methods are most effective in detecting defects located near the product surface.

- optic;

- **acoustic** - this method is based on recording the parameters of elastic waves created in a controlled object;

- **penetrating substances** - this method is based on the capillary penetration of substances into the defect cavities of the controlled object.

Depending on the location of possible defects, they can be conditionally divided into surface, subsurface with a depth of 0.5 to 1.0 mm and internal with a depth of more than 1.0 mm. All methods are applicable to detect surface defects, but the most effective of them are visual-optic, magnetic particle and capillary. To detect subsurface defects, ultrasonic, eddy current, and magnetic particle are effective. To detect internal defects, it is better using ultrasonic methods.

3. Analytical study and computer-aided simulation of dynamic properties of aircraft component in full-scale test

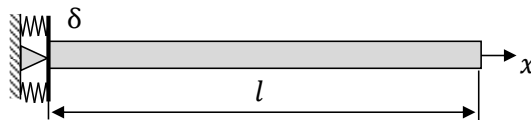
The chapter is based on research presented in the article "On the Dynamic Response Prediction at the Full-Scale Test of Aircraft Component" [62].

3.1. On the Properties of Solutions of the Structural Dynamics of Elastic Systems

The general solution of the linear dynamic problem of an elastic system is described by a system of ordinary differential equations or partial differential equations. Each such set of equations has an infinite number of solutions, among which there is a unique solution to a specific problem. It is determined by the boundary conditions. In other words, the properties of the external and internal constraints are determined by the external supporting and interaction between the parts of the dynamic system. For example, for the one-dimensional problem, the number of permanent integration coincides with the number of superimposed ties. In the practice of real system analysis, the properties of the boundary conditions are often simplified: absolutely rigid supports, perfectly smooth contact surfaces (frictionless). These are the so-called classical boundary conditions. Obviously, the real systems do not have any classical boundary conditions. In each case, the effects of possible deviations should be evaluated. If necessary, the boundary conditions can be described in more detail to provide a correct result.

This paper analyses the ways of obtaining the estimates of the effect of boundary conditions and some general regularities of this effect.

3.2. Simple Example: A Cantilever Beam With an Elastic Clamping



3.1. Figure. A cantilever beam with an elastic rotational support.

In this example, the analysis of the system permitting a simple analytic solution is carried out. It allows to show some general regularities of the effect of boundary conditions to the dynamic characteristics of the elastic system.

The transverse free oscillations of the thin uniform beam with elastic support are analysed.

The solution of a differential equation of the beam bending allows to obtain the general solution of the beam shape $V(x)$ of the normal vibration mode

$$V(x) = C_1 \cosh kx + C_2 \sinh kx + C_3 \cos kx + C_4 \sin kx, \quad (3.1)$$

where k is a root of characteristic equation.

The integration constants C_1, C_2, C_3, C_4 are defined by the boundary conditions. For the cantilever beam (Fig. 3.1), they can be expressed as follows:

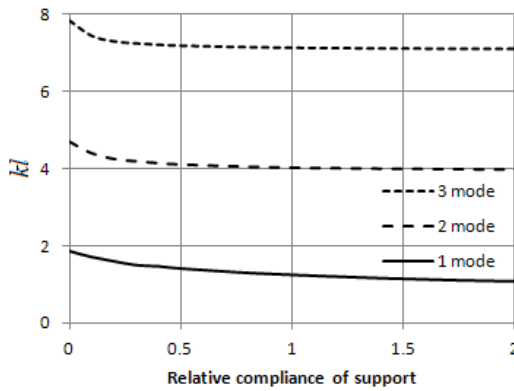
$$V(0) = 0, \quad V'(0) = \delta DV''(0), \quad V''(l) = 0, \quad V'''(l) = 0.$$

This creates a system of four linear homogeneous algebraic equations for determining the integration constants C_1, C_2, C_3, C_4 . This system has a non-trivial solution if the matrix of coefficients is equal to zero. The frequency equation in this case is:

$$\cosh kl \cos kl + \bar{\delta}kl(\cos kl \sinh kl - \sin kl \cosh kl) + 1 = 0, \quad (3.2)$$

where

- $\bar{\delta} = \frac{\delta}{l/D}$ is a relative compliance of the support;
- δ is a rotational compliance of the support;
- D is a bending stiffness of the cantilever beam cross-section.



3.2. Figure. Natural frequencies as functions of relative compliance of support.

disappears. Higher natural frequencies have nonzero limits, and for higher mode the rate of approaching to this limit is greater. In other words, if the mode of oscillation is higher, the natural frequency of this mode and its shape is less sensitive to a change of the elastic compliance of the support.

3.3. Dynamic Properties and Response of the Structure

Here is presented a general mathematical description of the complex elastic system that can be released by computational simulation for practical applications. Some elastic body or system of m bodies in the region $W = \cup_{j=1}^m (W_j)$ bounded by the external surface S are considered. Internal constraints are defined on the subbodies contact surfaces $S_{ij} = S_i \cap S_j$, and the external boundary conditions are given on the other part of surface S . The displacement vector $\mathbf{u}(\mathbf{x}, t)$ is defined by the following motion equation:

$$\rho(\mathbf{x})\ddot{\mathbf{u}}(\mathbf{x}, t) = L(\mathbf{u}) + \mathbf{p}(\mathbf{x}, t), \quad (3.4)$$

where

- $L(\mathbf{u})$ is a linear operator of the displacement vector $\mathbf{u}(\mathbf{x}, t)$;

The roots kl of the frequency equation define the spectra of beam eigenfrequencies.

$$f_n = \frac{(kl)_n}{2\pi l^2} \sqrt{\frac{D}{m}}, \quad (3.3)$$

where

- m is a mass of the beam unit length,
- $n = 1, 2, \dots$ is a number of the mode of oscillations.

In Figure 3.2, the natural frequencies as the function of elastic compliance are presented for the first three modes. A monotonic decrease of all natural frequencies is observed. If the compliance coefficient tends to infinity (disappearance of constraints), the first natural frequency tends to zero, so that the oscillatory form

$\mathbf{p}(\mathbf{x}, t)$ is an intensity of the excitation force;
 \mathbf{x} is a vector of coordinates of a point.
 For example, the operator $L(\mathbf{u})$ view of isotropic elastic body is

$$L(\mathbf{u}) = \lambda \operatorname{grad}(\operatorname{div} \mathbf{u}) + \mu \Delta \mathbf{u}, \quad (3.5)$$

where

λ and μ are Lamé constants.

The equation (3.3) can be resolved by the separated variables method in the following form:

$$\mathbf{u}(\mathbf{x}, t) = \mathbf{U}(\mathbf{x})\theta(t). \quad (3.6)$$

This solution exists if the function $\mathbf{U}(\mathbf{x})$ is some eigenmode of the next ordinary differential equation:

$$L(\mathbf{U}) + \omega^2 \rho(\mathbf{x})\mathbf{U}(\mathbf{x}) = 0. \quad (3.7)$$

The non-trivial solution $\mathbf{U}_k(\mathbf{x})$ (shape of the eigenmode) of equation (3.9) exists for some spectrum of eigenvalues (natural frequencies) ω_k , ($k=1, 2, \dots$).

At forced oscillation, the dynamic response of an elastic linear dynamic system under some external load can be described as a modal decomposition of the displacement vector $\mathbf{u}(\mathbf{x}, t)$ to the basic system of functions $\mathbf{U}_k(\mathbf{x})$ ($k=1, \dots, \infty$). As a result, the vector of displacements can be presented by series

$$\mathbf{u}(\mathbf{x}, t) = \sum_{k=1}^{\infty} \mathbf{U}_k(\mathbf{x})\theta_k(t), \quad (3.8)$$

where

$\theta_k(t)$ is a so-called normal function, which is a solution of the following ordinary differential equation:

$$M_k \ddot{\theta}_k(t) + M_k \omega_k^2 \theta_k(t) = \Phi_k(t), \quad (3.9)$$

here

$M_k = \iiint \rho(\mathbf{x})\mathbf{U}_k^2(\mathbf{x})dV$, $\Phi_k(t) = \iiint \mathbf{p}(\mathbf{x}, t)\mathbf{U}_k(\mathbf{x})dV$ is a modal mass of the system and a modal force respectively associated with the k -th mode of free oscillations.

The dynamic response $\mathbf{u}(\mathbf{x}, t)$ at a harmonic excitation by the force $\mathbf{p}(\mathbf{x}, t) = \mathbf{p}_0(\mathbf{x})e^{i\omega t}$ can be expressed by the following series:

$$\mathbf{u}(\mathbf{x}, t) = e^{i\omega t} \sum_{k=1}^{\infty} \frac{\mathbf{U}_k(\mathbf{x})\Phi_{k0}}{M_k(\omega_k^2 - \omega^2)}, \quad (3.10)$$

where

$\Phi_{k0} = \iiint \mathbf{p}_0(\mathbf{x})\mathbf{U}_k(\mathbf{x})dV$ and $\mathbf{p}_0(\mathbf{x})$ is an amplitude of modal force.

4. Vibration-based detection of structural damage in full-scale test

The chapter is based on the research presented in the article "Vibration-Based Detection of Small Damage in the Aircraft Large Component" [63].

4.1. Fundamentals of method (dynamic properties, dynamic response to different types of excitation, EMA and OMA approaches of dynamic properties evaluation and damage detection, board band excitation and frequency response function, transience function)

Vibration-based damage detection is one of the most attractive for structural health monitoring (SHM). Because modal characteristics of a structure are directly related to physical properties of the structure, (mass, stiffness, and damping) then they can be used to detect, locate, and characterize damage in the structure [27]. There are large number of research and developments in mechanical, civil, and aerospace engineering dedicated to vibration-based damage detection. Some corresponding review-information can find in [2-8,28]. Methods that use changes of natural frequencies due to presence of damage usually require simple vibration measurements for estimation of position and growth of damage after calibration or accurate physics-based simulation. The mode shapes directly provide also spatial information of structural changes due to damage. Curvature mode shapes can be more sensitive and more effectively used to identify damage [29, 30].

Two basic techniques are used for practical realising of the vibration-based damage detection. Traditional is the experimental modal analysis (EMA) that allows more complete and accurate to identify damage. However, the EMA requires the measurement of both the input and the output of dynamically loaded structure. Other the operational modal analysis (OMA) uses output only, is cheaper and faster than EMA and can be easily applied to large structure [14].

In the presented paper there are investigated the principal problems of the local system of SHM of large scale aircraft component. Vibration-based damage detection is accepted as a basic condition, and main attention focused to a low-cost solution that would be attractive for practice.

4.2. General problems of vibration based method (VBM) application

The global aim of research is a problem of vibration-based method of NDT application for SHM based on some solution for a relatively small structural damage detection using operational low-frequency excitation (OMA approach).

It is known, the direct modal analysis is or low sensitive or difficult for practical application in operation. If the scale of damage is small in comparison with structure dimensions, then effect of damage is significant only for higher modes of structure. For example, there are number of analytical and experimental investigations of crack or additional small mass effect to dynamic properties of the cantilever beam [31-36] those confirm appreciable shift of separate higher natural frequencies only and change of corresponding mode shapes. Later ones show location of damage, but for the reliable indication of damage the branched net of sensors is needed.

But theoretically any response of linear dynamic system is a linear combination of all modes. The principal question: is effect of damage sufficient for its detection of the available vibration-based technique of NDT? Other question is associated with the fitness of this technique for implementation in the SHM system. Some acceptable solution can be find, if its application will be a priori restricted by some conditions. The main of them is restriction of dimensions of monitored zone of structure. By other words the SHM system should be local. Second condition accepted in this paper: the SHM system should be objectively oriented (the type of damage, its location, acceptable detectable size should be known). At those conditions the local vibration-based SHM system can be developed and has some perspective of practical application in operation.

More detailed description of investigation aim is followed.

There is a large full-scale component of some structure. In fixed zone of structure a structural damage is expected. A few sensors are embedded in this zone for vibration measurement at low frequency excitation. More precise, the excitation basic frequency is close to the first natural frequency of full structure and is much smaller than the first “local” natural frequency of a monitored zone. The investigation of this problem and development of some approach of extraction of damage features is detailed aim of presented paper.

4.3. The basic idea of innovative approach of a damage detection by VBM: the use of group evolution of higher modes

The effect of damage to dynamic properties of a structure was estimated by general linear model of structure with embedded small 1D oscillator. Latter one is simulated the local mass/stiffness variation of structure parameters due to a damage. Finally, the dynamic response of linear system at harmonic excitation can be presented in equation (4.3.1).

$$\mathbf{u}(\mathbf{x}, t) = \sum_{k=1}^{\infty} \mathbf{U}_k(\mathbf{x})\theta_k(t) \quad (4.3.1)$$

where $\mathbf{U}_k(\mathbf{x})$ and $\theta_k(t)$ are the modal vector and the normal function of the k^{th} mode of free oscillation. Note that the modal vector corresponds to intact structure.

At harmonic excitation with a circular frequency ω the normal function of the k^{th} mode is:

$$\theta_k(t) = A_k(\omega)e^{j\omega t} \quad (4.3.2)$$

$$A_k(\omega) = \frac{(1 - \bar{\omega}^2)\Phi_k}{[M_k(1 - \bar{\omega}^2) + m(\boldsymbol{\xi}_0)\mathbf{u}(\boldsymbol{\xi}_0)\mathbf{U}_k(\boldsymbol{\xi}_0)](\omega_{dk}^2 - \omega^2)} \quad (4.3.3)$$

where M_k and $\Phi_k = \iiint \mathbf{F}_0(\boldsymbol{\xi})\mathbf{U}_k(\boldsymbol{\xi})dW$ are the modal mass and modal force of the k^{th} mode. The modal frequency of damaged structure ω_{dk}^2 is defined in equation (4).

$$\omega_{dk}^2 = \omega_k^2 \left[1 + \frac{m(\boldsymbol{\xi}_0)\mathbf{u}(\boldsymbol{\xi}_0)\mathbf{U}_k(\boldsymbol{\xi}_0)}{M_k(1 - \bar{\omega}^2)} \right]^{-1} \quad (4.3.4)$$

here $\mathbf{u}(\boldsymbol{\xi}_0)$ is a vector-amplitude of oscillation of main structure in a base of oscillator. Excitation relative circular frequency $\bar{\omega}$ is given in respect to the natural frequency of oscillator.

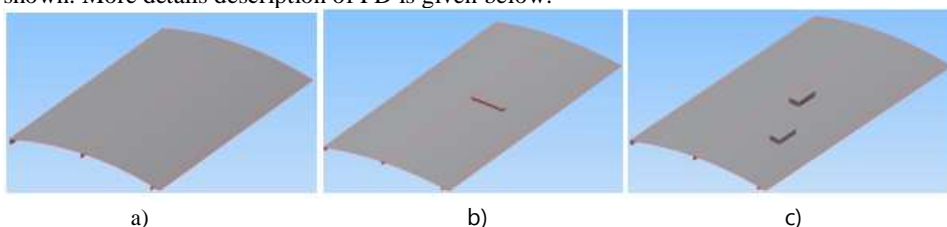
Equations 3 and 4 define the effect of damage to modal frequency and amplitude of harmonically forced vibration. From equation 4 it is seen that this effect can be appreciable only for mode with modal and excitation frequencies close to the natural frequency of oscillator and at the condition that

the mass of equivalent oscillator is not very small in comparison with modal mass M_k . The effect of damage is more complex and defined by variation of modal frequency and modal mass.

So the effect of small damage practically cannot be reliably detected at low-frequency excitation in conditions of formulated problem using only modal analysis of output signal. However, in practice, the input signal often contains high-frequency components (for example, white noise). In this case, high eigenfrequencies due to local design properties of structure can be detected in the spectral decomposition of the output signal. Obviously that a small-size defect most significantly affects the dynamic response of the structure in the damaged zone. For this purpose, an analysis of the local dynamic properties of the object of investigation was carried out. The tested tail beam has a thin-walled quasiperiodic structure. Its elementary structural unit is the skin fragment bounded by two adjacent stringers (in the circumferential direction) and two adjacent frames (in the longitudinal direction).

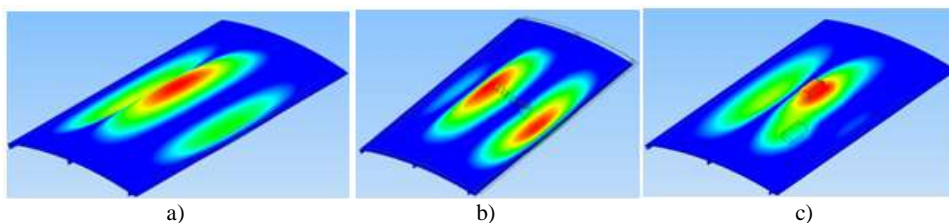
Below there is presented the results of a local modal analysis of small 0.5 mm thin-walled panel of the tail beam. The cylindrical panel with 450 mm of curvature radius simulates a portion between two frames (distance 372mm) and cover three stringers (figure 1, a). Total length of a curved edge of a panel is equal to 218 mm. The pin-type boundary condition is selected at all contour of a panel. As a result, the conditions of dynamic behaviour of middle stringer and close part of a skin were estimated as similar to the same part in assembled structure. The Autodesk Inventor was used for both geometrical simulation and modal FEA.

In figure 4.1 the CAD model of a panel, and its views with two types of pseudo-damage (PD) are shown. More details description of PD is given below.



4.1. Figure. The model of a panel for intact structure (a) for the SPD, (b) for the LPD.

Several results of modal FEA are presented in figure 4.2. First natural frequency is equal to 367.91 Hz for intact panel, 383.08Hz for SPD, and 274.63 Hz for LPD.



4.2. Figure. The first mode of a panel for intact structure (a) for the SPD (b), and for the LPD (c).

So, a small damage of structure is able appreciably affect to local dynamic properties of some small part of structure. It is seen also that such damage effect to general dynamic properties of a structure is limited by the local changing of shape of the mode which natural frequency is closest to local natural frequency of damaged zone.

5. Experimental study and method validation

The chapter is based on the research presented in the article "Vibration-Based Detection of Small Damage in the Aircraft Large Component" [63] and on the research of the author of the tail boom of the Ka-62 helicopter on a special stand in the "Aviatest" laboratory [67].

5.1. Full-scale comp used in the test

5.1.1. Study on the tail boom of the Mi-8 helicopter

Short description of the full scale structural component of aircraft

The helicopter Mi-8 tail beam structure was selected for experimental investigation (general view in figure 5.1). The beam has the form of the truncated cone with a length of 5485 mm, and the diameters of end cross-sections are 1000 and 550 mm respectively. The material of all main elements of the beam is the aluminium alloy D16AT (close to Al2024-T3). A skin thickness is in interval 0.5-0.8 mm. Stringers (total number 26 ones) of angular cross-section are connected to the skin by spot-welding. The 17 frames are riveted to the skin. There are number of non-regularities of structure of the beam due to technological and operational requirements (hatches, connection units, transmission supports, etc.) that are the potential sources of skin damaging in operation.



5.1. Figure. General view of the helicopter Mi-8 tail beam (a) and the test setup for dynamic loading (b), 1- the tail beam, 2- imitator of the tail rotor beam, 3 – the eccentric shaker.

5.1.2. Study on the tail boom of the Ka-62 helicopter

For the experimental investigation of the dynamic response to pulsed excitation, the tail boom structure of the Ka-62 helicopter was used.

Figure 5.2 shows the tail boom in the design of the Ka-62 helicopter (structural groups).

The general view of the beam on the test bench is shown in Figure 5.3



5.2. Figure. Constructive groups of the Ka-62 helicopter



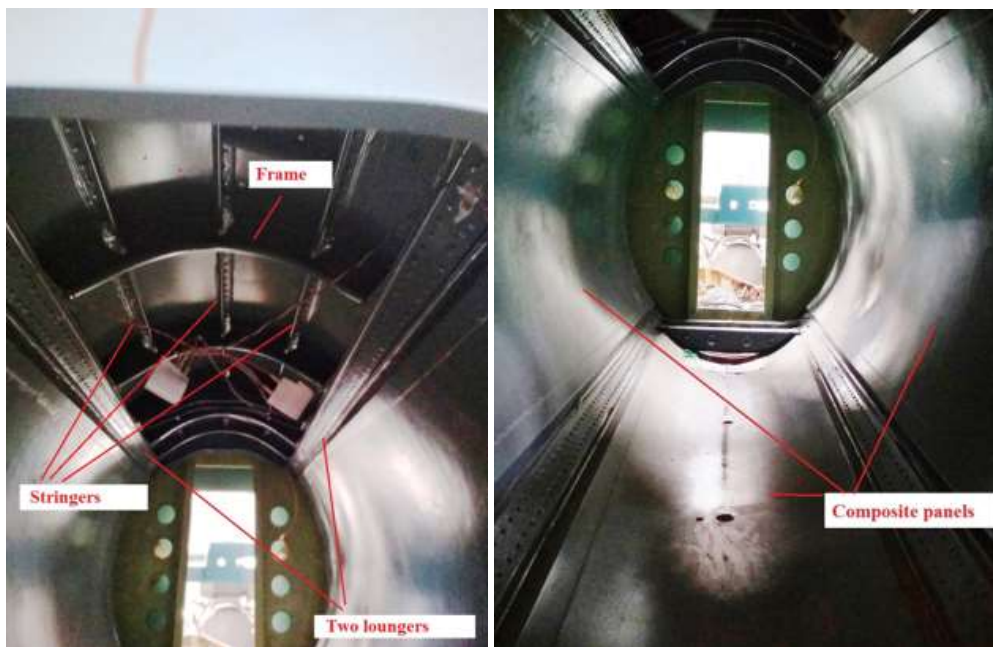
5.3. Figure. The tail boom of the Ka-62 helicopter on the test bench

The beam has the shape of a truncated cone.

Geometrical parameters of the tail boom:

- length 2.70 m;
- a larger diameter of 1.05 m;
- smaller diameter 0.61 m.

The power set of the beam is a skin, spars, stringers. The material of these elements is aluminum alloy D16. The thickness of the skin is 0.8 mm. Four spars are located at an angle of 45 degrees to the vertical line. Three stringer are located between the upper spars (Figure 5.4a). A special feature of the design of the tail boom of the Ka-62 helicopter is the use of composite panels. Composite panels are installed inside between the side members in the side and the bottom (Figure 5.4b). Composite panels are connected to the skin by rivets. The thickness of the plating package and composite panel is 10 mm.



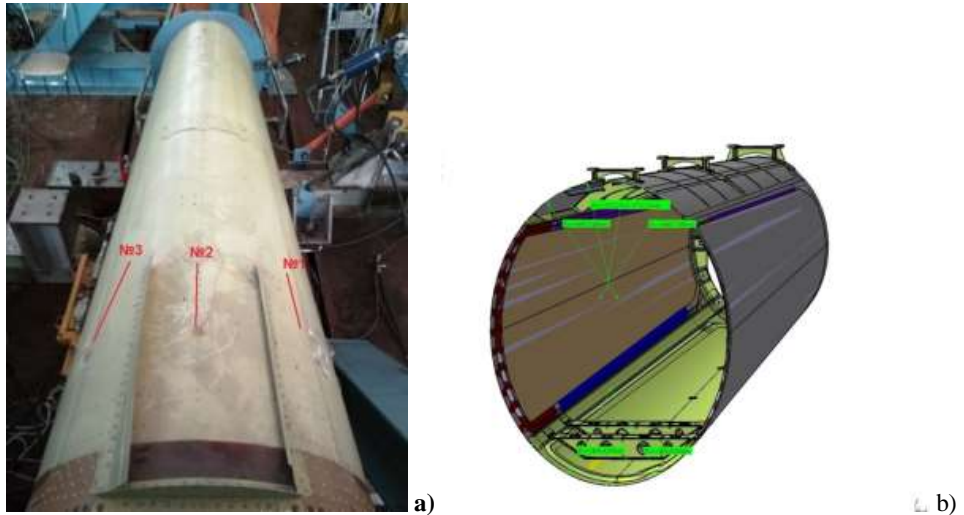
a)

b)

5.4. Figure. Power beam set

To obtain a signal from the impulse action on the tail boom, there are three strain gauges (Fig. 5.5a). In the figure, numbers 1, 2, 3 show the location of the strain gauges.

Based on the geometric data, a computer model of the beam box is compiled to determine the expected frequencies at which the response can be obtained (Fig. 5.5b). Impulse action on the beam was in the form of a shock in the vertical plane on the flange in the end part of the beam.



5.5. Figure. Location of strain gauges (a) and computer model (b)

To obtain a diagnostic test for impulse action, the method of loosening the bolted joint at the junction of the tail boom and the fuselage was used. At the stand, the fuselage was imitated by a bench plate. Figure 5.6 shows the places of weakness of bolted connections.



5.6. Figure .The place of easing of the tightening of bolts in the flange connection of the tail boom and fuselage. a) view of the direction of flight; b) view versus flight

5.2. The objective of test and equipment

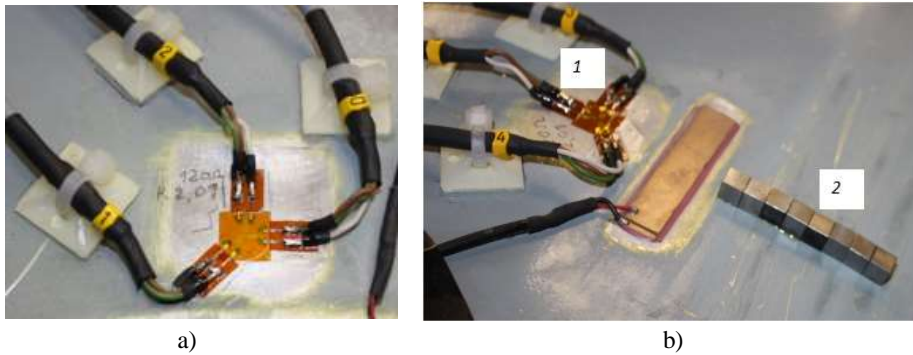
5.2.1. The objectives of test

- 1) Measurement of the strain/stress state of some aircraft full-scale component at dynamic loading.
- 2) Experimental investigation of pseudo-damage effect to the strain/stress state of skin of the tail beam at nominally harmonic excitation.

5.2.2. Test setup

Test setup contents the test portal as a base for fixing of the tail beam, the imitator of the tail rotor beam, and the eccentric shaker with electromechanical drive (figure 5.1, b).

In contrast to usual practice of vibration test, the strain gauge technique was used for the dynamic



5.7. Figure. A rosette of three strain gauges (a) and a strain gauge rosette with the small pseudo damage (SPD) in zone 2 (b).

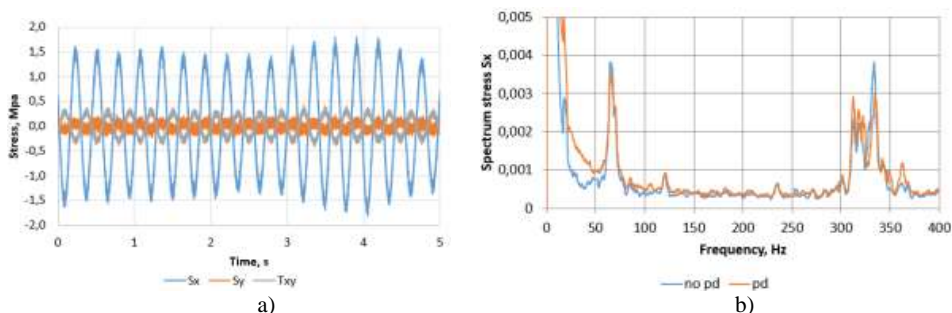
measurement. Two strain gauge rosettes were pasted in two zone of the outer surface of a skin. In the Figure 5.7, a the rosette in the zone 2 is shown.

The technology of pseudo damage was used for damage effect simulation. Pseudo damage is a non-destructive modification of a test object which affects local dynamics properties of a testing structure [19-21]. The small pseudo damage (SPD) was completed as row of eight 6×6×6mm steel blocks (total mass 12 g) and placed in the zone 1 (figure 5.7, b). Two steel blocks (total mass 26 g) were pasted in the zone 2 and qualified as large pseudo damage (LPD).

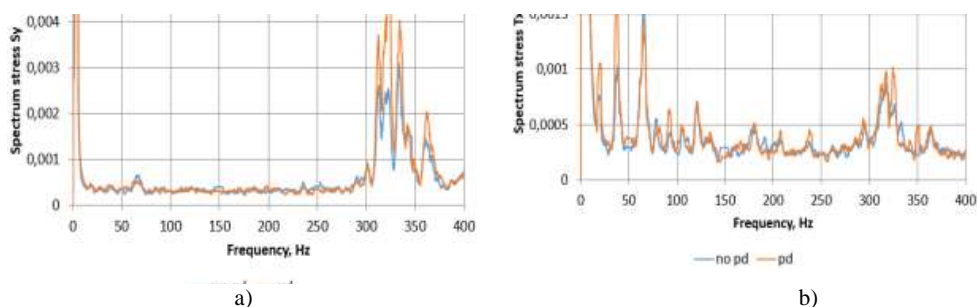
Dynamic strain was measured by the multichannel oscilloscope NI PXIe-4330, 16Ch, 24-Bit, 25 kS/s Bridge Input Module and PC with NI LabVIEW software. The sampling rate 5 kS/s and the length of a record in 5s were accepted as optimal for the data acquisition sufficient for the aim of experimental study. Cyclic excitation of vibration was limited by frequency band close to the first natural frequency of a beam (3.9 Hz).

5.3. Test results

The main results of test for excitation frequency 3.8 Hz is presented below. Using strain measurement data, the components of plain stress state σ_x , σ_y , τ_{xy} were defined in both zones. It is



5.8. Figure. The components of stress state in the zone 1 as time functions (a) and spectrum of stress component σ_x in the frequency band 0-400Hz in the zone 1 (b).



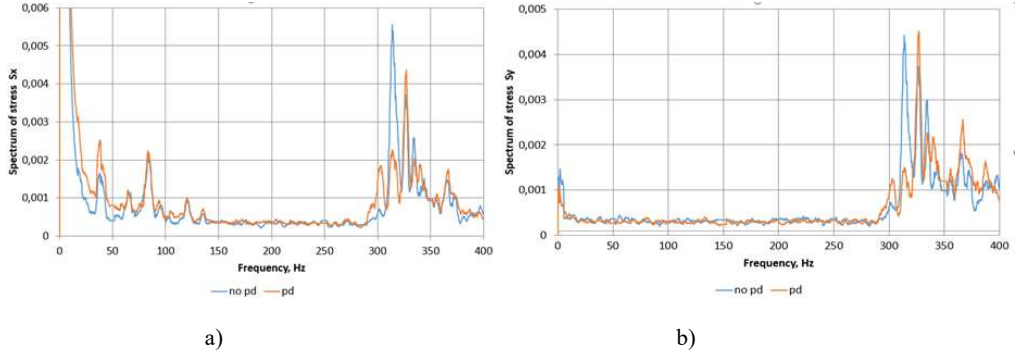
5.9. Figure. Spectrum of stress component σ_y (a) and stress component τ_{xy} in the frequency band 0-400Hz in the zone 1.

accepted that the axis x coincident with longitudinal direction of a beam and the axis y is perpendicular to first one.

Typical stress/time functions are shown in the figure 5.8,a for stress state in the zone 1. Fast Fourier transform (FFT) was done for each of three stress components (figures 5.8b; 5.9 a, 5.9, b) for intact and structure with a pseudo-damage. Similar results for zone 2 with LPD are presented in figures 5.10. Spectral transform allows to define directly the resonance frequencies 3.9, 20.6, 38.6, 65.0 Hz that was confirmed also by the direct measurement in process of dynamic test. Significant peaks of spectrum are also at frequencies 83.8, 121.2, 136.6 Hz. It can be seen that any shift of mentioned resonance frequencies is not observed at presence of PD. In the frequency band 150-275 Hz the amplitude of spectrum is distributed with relatively small fluctuation. Amplitude of spectrum sharply increases in the frequency band 275-400 Hz.

The spectrum of all components of stress for structure with PD is close to corresponding spectrum of the intact structure.

Interesting result is obtained for the spectrum of stress component σ_y (lateral direction): the amplitude of spectrum is large practically in the frequency band 275-400 Hz only (figure 5.10, b).



5.10. Figure. Spectrum of stress component σ_x (a) and stress component σ_y (b) in the frequency band 0-400Hz in the zone 2.

5.4. Discussion and feature extraction

As noted above, the tested beam has a quasiperiodic structure. Therefore, it can be assumed that there is an interaction of neighboring structural units and the existence of many eigenmodes of the beam vibration in a narrow frequency band. Indeed, an additional modal analysis of the more complex part of the beam that consists 39 structural units shows that there are at least fifteen independent eigenmodes in the frequency band 280-390 Hz. In the same limits, intensive increasing of response spectrum is observed in test (figures 5.8-5.10). This can be explained by the presence of a close spectrum of natural frequencies in the band 275-400 Hz.

At the same time, changes in the spectral power of response due to the appearance of damage can be seen. Moreover, the complexity of the dynamic response spectrum in the frequency band of interest causes difficulties of defect identification by the shift of the natural frequency and the change in the shape of the modes.

Therefore, variants of the integral estimation of the change in the response spectrum were considered. The most successful is the use of the correlation coefficient deviation (CCD) index that is widely used in different applications [22-25].

$$CCD = 1 - CC \quad (5.1)$$

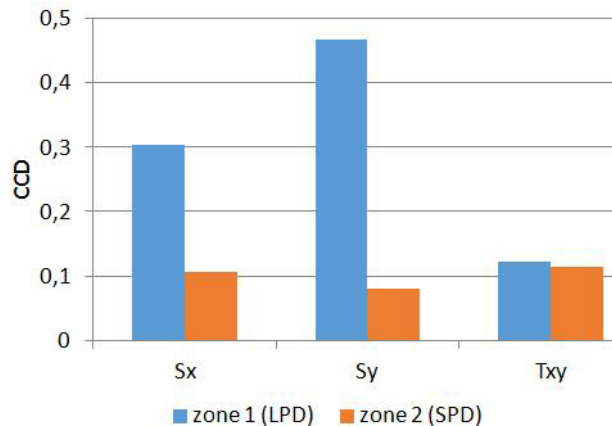
where

$$CC = \frac{cov(x, y)}{s_x s_y} \quad (5.2)$$

$cov(x, y)$ is the covariance between two sample random vectors x and y those are the spectrum of response of intact and damaged structures respectively in selected frequency band, and s_x, s_y are the standard deviations of random vectors. It is seen that the CCD index is equal to zero, if there is not any damage effect, and cannot be more than 1. The larger value of the CCD index corresponds to higher effect of damage.

In figure 5.11 the comparison of CCD indices of damaged (with LPD and SPD) structures are shown for the spectrum of dynamic response at excitation nominal frequency 3.8 Hz. It is seen that the CCD index increment due to pseudo-damage is observed for all stress components. At the same time, the damage effect is greater for a larger pseudo-defect.

The important aspect of this index application is the requirements to input signal. A general assumption in the theory of OMA concerns the input which is not measured and consists of a Gaussian white noise with a flat spectrum in the frequency band of interest [12]. At the nominally harmonic excitation with frequency close to



5.11. Figure. Effect of pseudo-damage to CCD index

first resonance the intensities of output for intact and damaged structures may be different. Therefore, the processing of each record of the output signal must provide of its normalization before the operation of determining the index. The mean amplitude of output was used here as acceptable estimate of output intensity.

6. Statistical Estimation of Perspective Damage Index for Vibration-Based Structural Health Monitoring

The chapter is based on the research presented in the article "Statistical Estimation of Perspective Damage Index for Vibration-Based Structural Health Monitoring" [65].

6.1. About Test Setup and Measurement Equipment

The helicopter Mi-8 tail beam structure was selected for experimental investigation (p.5.2.2).

The strain gauge technique was used for the dynamic measurement. Two strain gauge rosettes were pasted in two zones of the outer surface of a skin (figure 5.7). Dynamic strain was measured by the multichannel oscilloscope NI PXIe-4330, 16Ch, 24-Bit, 25 kS/s Bridge Input Module and PC with NI LabVIEW software. The sampling rate 5 kS/s and the length of a record in 5s were accepted as optimal for the data acquisition enough for the aim of experimental study.

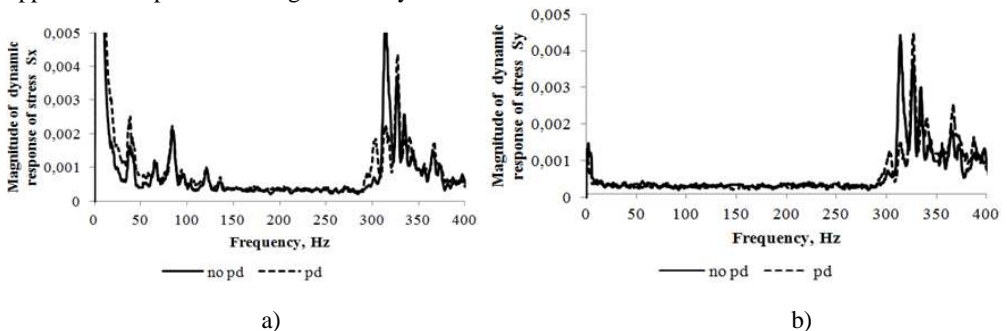
The forced vibration of the beam was excited by the mechanical eccentric shaker with control of excitation frequency. In the below presented analysis there are used the dynamic responses of a beam at the cyclic excitation with basic frequency 3.55 Hz (close to the first natural frequency of a beam) and low amplitude vibration in the frequency band of interest (white noise).

The technology of pseudo damage was used for damage effect simulation. The small pseudo damage (SPD) was completed as row of eight 6×6×6mm steel blocks (total mass 12 g) and placed in the zone 2 (figure 5.7, b). Two steel blocks (total mass 26 g) were pasted in the zone 2 and qualified as the large pseudo damage (LPD).

6.2. Some Important Results of Research

The dynamic response in frequency domain was obtained for each stress components (two examples for σ_x and σ_y in the figure 6.1) for intact (solid) and structure with a pseudo-damage (dash). It can see that in the frequency band 275-400 Hz there are observed multiple resonances.

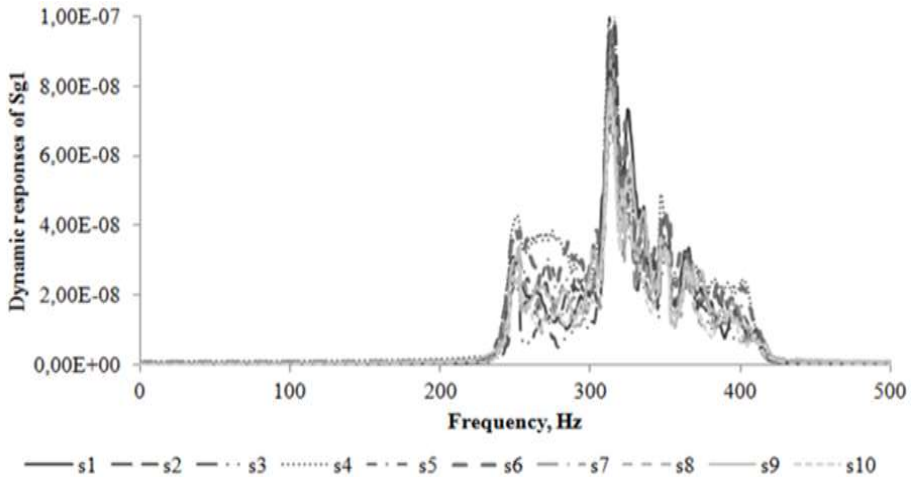
The stress component σ_y spectrum is especially interesting. In the relatively low frequency band, the frequency response is very weak. And in the above-mentioned frequency band there is a sharp increase in the spectrum. Moreover, for all components of the stress tensor, the response to the appearance of pseudo-damage is clearly observed.



6.1. Figure. The dynamic response of stress component σ_x (a) and σ_y (b) in the frequency band 0-400Hz in the zone 1

6.3. Data Acquisition and Statistical Analysis

To obtain the test data for the statistical analysis there was carried out on 10 series of measuring of dynamic strains at the checkpoints of the intact structure and in the presence of pseudo-damage. Time record length was chosen to be 1 second at sampling frequency of 5000 points. Pre-processing of each record includes signal centring and filtering in the frequency band 250-400 Hz. The band pass filter was designed by IIR method (Butterworth). Fast Fourier transform (FFT) and light smoothing (with span 7) of frequency response function was done at the final step of pre-processing. As a result, ten samples of the dynamic frequency response were obtained for each of six strain gauges. Example of this type outcome for the longitudinal strain gauge of zone 1 is presented in figure 6.2.



6.2. Figure. Frequency response of the strain gauge sg1 after filtering and FFT (intact structure)

The data set for final statistical analysis contents two set for each of the strain gauges. The set size is ten observations, each of which represents the frequency response in the band 250-400 Hz and has a size of 500 points.

The matrix $A_k(500,10)$ contents ten observations of the intact structure frequency response measured by the strain gauge k , and the matrix $B_k(500,10)$ is the same for pseudo-damaged structure.

The final statistical analysis consists three steps.

Step 1: Analysis of the inter-sensor correlation in a separate loading session. In such case, the dynamic response of all strain gauges is caused by the same external load. This means that in a linear system, the strain components must be strictly proportional to each other, and the correlation coefficient between them must be 1. Deviation from 1 may be caused by the influence of the measurement accuracy and/or nonlinearities of a structure.

The correlation coefficient $C_{km}^{(n)} = \text{corrcoef}(A_k(:,n), A_m(:,n))$ between random variable $A_k(:,n)$ and $A_m(:,n)$ of observation (test option) n was calculated for intact structure, and

similarly, for pseudo-damaged structure $C_{km}^{(n)} = \text{corrcoef}(B_k(:, n), B_m(:, n))$. For strain gauges of zone 1 $k = 1$ and $m = 2, 3$, and for zone 2 $k = 4$ and $m = 5, 6$, $n = 1, 2, \dots, 10$.

Outcome of this analysis is presented in the Table 6.1.

6.1. Table
The mean and minimum values of the correlation coefficient

State of structure	Value of parameter	C_{12}	C_{13}	C_{45}	C_{46}
Intact	Mean	5	5	9	9
	Minimu m	4	4	1	1
Pseudo- damage	Mean	7	6	1	0
	Minimu m	9	0	5	2

The mean value of correlation coefficient for all data set is equal to 0.99997, and the minimum is 0.99987. It means that the inter-sensor correlation in a separate loading session is very close, the accuracy of the measurements is relatively high, and the effect of nonlinearities is insignificant.

Step 2: Estimation of load scattering effect to the dynamic response of a separate strain gauges and the distribution law of CCD. The mean vectors of all observations for each strain gauge was obtained for both intact and pseudo-damaged state of a structure.

$$\bar{A}_k = \sum_{n=1}^{10} A_k(:, n) \quad \bar{B}_k = \sum_{n=1}^{10} B_k(:, n) \quad (6.1)$$

The correlation coefficients

$$C_{k0}^{(n)} = \text{corrcoef}(A_k(:, n), \bar{A}_k) \quad C_{k1}^{(n)} = \text{corrcoef}(B_k(:, n), \bar{B}_k) \quad (6.2)$$

and the correlation coefficient deviation (CCD)

$$CCD_{k0}^{(n)} = 1 - C_{k0}^{(n)} \quad CCD_{k1}^{(n)} = 1 - C_{k1}^{(n)} \quad (6.3)$$

can be introduced as the signatures of deviation of any observation from averaged value due the specific load at given state of a structure. The mean values of the CCD for all six strain gauges are presented in the Table 6.2.

6.2. Table
The mean values of the correlation coefficient deviation of dynamic response

State of structure	sg1	sg2	sg3	sg4	sg5	sg6
Intact	0.04147	0.03588	0.06115	0.10023	0.04093	0.05373
Pseudo- damaged	0.21180	0.10863	0.06877	0.13966	0.04489	0.05579

Thus, estimates of the effect of load variation to CCD index were obtained for two states of system. At the same time, the installation of pseudo-damages led to an increase of CCD for two sensors in the LPD zone, which indicates the effect of a configuration change on the dispersion of CCD due to the variation in load.

The null hypothesis that the data in vector-column in CCD_0 and CCD_1 matrices is from a population with a normal distribution in seven tests from twelve were rejected by the Anderson-Darling test. Thus, there is not reliable evidence about normal distribution of considered random variables.

Step 3: Features extraction. The damage index CCD corresponding to the strain gauge k frequency response in the observation n is defined by equation (6.4)

$$CCD_k^{(n)} = 1 - C_k^{(n)} \quad (6.4)$$

The correlation coefficient $C_k^{(n)}$ between the dynamic response of the pseudo-damaged structure in the frequency band of interest $B_k(:, n)$ measured by the strain gauge k in the observation (test option) n , and the average response \bar{A}_k of this strain gauge in the intact structure.

First of all, a test decision for the null hypothesis that the random vectors $B_k(:, n)$ and \bar{A}_k are from the same continuous distribution was done using the two-sample Kolmogorov-Smirnov test. Data set of this test decision for pseudo-damaged structure defined by equation (5) are represented in the Table 6.3.

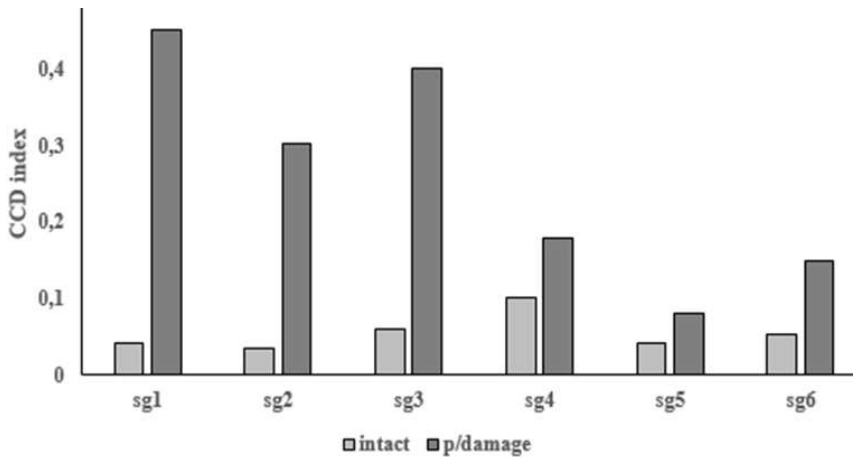
For five tests (sg1, sg2, sg3 – zone 1 of LPD and sg5, sg6 – zone 2 of SPD) the null hypothesis was rejected at the 5% significance level. Only for one test (sg4 - zone 2 of SPD) null hypothesis was not rejected. This means that the CCB index uniquely detects the appearance of a LPD. Effect of the SPD to CCD is significantly weaker that bear witness to the effectiveness of the proposed index.

6.3. Table

Data set for CCD random variables of the strain gauges.

Number of test	sg1	sg2	sg3	sg4	sg5	sg6
1	0,7010	0,3969	0,3682	0,1957	0,0928	0,1214
2	0,4260	0,2185	0,4995	0,1307	0,0549	0,2303
3	0,2003	0,2029	0,4052	0,0886	0,0580	0,1033
4	0,3606	0,1160	0,4448	0,1663	0,0475	0,0664
5	0,5063	0,2449	0,3808	0,2812	0,1146	0,2016
6	0,3484	0,3547	0,3445	0,2120	0,0795	0,1439
7	0,3124	0,1567	0,4091	0,0979	0,0592	0,1317
8	0,6805	0,3026	0,3668	0,3237	0,1437	0,1437
9	0,6496	0,8709	0,4902	0,1227	0,0410	0,1022
10	0,3208	0,1594	0,3042	0,1674	0,1243	0,2415
Mean	0,4506	0,3023	0,4013	0,1786	0,0815	0,1486

Comparison of the mean value of CCD indices of intact and pseudo-damaged structures is represented in Fig. 6.3. This index of intact structure is associated mainly with the variation of the external load in different test options, but the index of pseudo-damaged structure mainly caused by a pseudo-damage effect. It is seen that for all three strain gauges (sg1, sg2, and sg3) located in the zone 1 the significant increment of CCD index is observed that due to presence of the large pseudo-damage. The small pseudo-damage in zone 2 also induces increasing of CCD index of all three strain gauges (sg4, sg5, and sg6), but effect of SPD is much less.



6.3. Figure. The mean value of CCD indices of intact and pseudo-damaged structure

7. An example of the test facility development with an analysis of its dynamic strength and elements of built-in continuous monitoring of the technical state of the test facility and object

The chapter is based on the author's research at the stand "Full-size stand of the Ka-62 helicopter" [66].

Creating a stand model and a system for monitoring the state of the stand allows you to obtain the dynamic characteristics of the stand in operating modes. This allows you to carry out the necessary improvements to the stand to improve its characteristics. The bench state monitoring system is a source of diagnostic signals during its operation.

7.1. Main priorities and stages of test facility creation

Regardless of the specific task of ground strength testing of full-size components of aircraft structures, a typical test procedure includes the following main stages:

1. Study of the Customer's technical requirements.
2. Facility design.
3. Manufacturing and installation of facility components.
4. Test object installation on the facility.
5. Test mode debugging.
6. Testing.
7. Processing of test results.

The example below focuses on describing those stages of actual tests that reflect the practical implementation of the proposals specified in this work:

1. Static and dynamic strength calculation of the test facility and object under all loading conditions stipulated by the program. Weak points of the test complex were identified and design improvements were recommended.
2. Modal analysis of the test complex in order to identify dangerous dynamic loading modes, as well as creating a system for built-in continuous monitoring of technical state of the test facility and object based on vibration analysis.

7.2. Facility creation purpose

A full-size facility (FF) is designed to test the drive system, the main and tail rotor of the helicopter, including:

- main gearbox;
- tail gearbox;
- main shafts;
- tail shaft;
- main rotor hub;
- main rotor swashplate.

7.3. Purpose of the main parts of the facility

Generally, the facility consists of the following main parts:

- power frame fixed to the power foundation;
- system for load application to the test object;
- facility measurement systems.

In this case, the facility includes:

- helicopter fuselage modified for attachment to the power frame;
- remote control system for starting, operating modes and shutdown of engines;
- remote control system of the main rotor, tail rotor and main rotor brake;

The power frame is designed for:

- installation of the test object in a fixed position for all test modes stipulated by the test program;
- installation and maintenance of elements of the load application system for power loading of the test object.

The load application system is designed to control the power loading process of the test object. The system is controlled remotely according to a previously entered program from a computer of the control system. The system has control and executive elements. It is usually fixed on a power frame during the final assembly of the facility.

The facility measurement system is intended for fixing the test object parameters and facility structure. At the moment, the systems based on obtaining information from strain gauges, vibration and displacement sensors are often used in tests related to the object strength assessment. The system has a computer with a corresponding data gathering program.

The helicopter fuselage is part of the test facility, since the main gearbox, the tail rotor drive system and the carrier system are tested.

7.4. Technical requirements for facility design

7.4.1. Helicopter

The helicopter fuselage was made for testing according to the design documentation. Additional fasteners are installed on the fuselage at the connection points with the facility power frame.

The test object is installed on the fuselage, consisting of:

- main gearbox;
- tail gearbox;
- main shafts;
- tail shaft;
- main rotor hub;
- main rotor swashplate,

therefore, the fuselage is an integral part of the test facility.

7.4.2. Power frame

Particular attention in the Terms of Reference is given to the power frame.

In addition to the requirements related to the convenience of helicopter maintenance during testing, the power frame should withstand the loads transmitted from the test object to the helicopter. The Terms of Reference indicate the design cases of the facility structure loading (see Table 7.4.1). When designing the power frame, the calculation of its strength and dynamic properties was carried out for design cases according to Table 7.4.1.

7.4.1. Table

Design cases of the facility structure loading

No.	Case name	Loads*	Safety factor
Effect of operational loads			
1	Maximum vertical thrust of the main rotor	$T_{mr} = 8,500 \text{ kg}$	$K = 4$
2	Maximum horizontal component of the main rotor thrust directed forward	$0.15T_{mr}$	$K = 4$
3	Maximum horizontal component of the main rotor thrust directed backward	$0.15T_{mr}$	$K = 4$
4	Maximum horizontal component of the rotor thrust directed sideward	$0.075T_{mr}$	$K = 4$
5	Maximum torque for the right (left) turn (effect of the tail rotor thrust)	$V_{tr} = 750 \text{ kg}$	$K = 4$
Loads during emergency operation of the facility			
6	The case of one rotor blade detachment: effect of the centrifugal force in the main rotor rotation plane (at the nominal rotation speed of the main rotor shaft $n_{nr} = 305 \text{ rpm}$)	$N_{ctmr} = 27,870 \text{ kg}$	$K = 2$
7	The case of one tail rotor blade detachment: effect of the centrifugal force in the main rotor rotation plane (at the nominal rotation speed of the tail rotor shaft $n_{tr} = 2,796 \text{ rpm}$)	$N_{ctr} = 2,540 \text{ kg}$	$K = 2$

7.5. Calculation of the facility strength and dynamic parameters

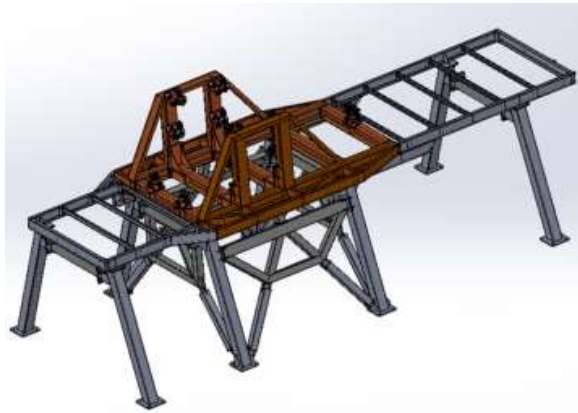
7.5.1. Work purpose, initial information features and problem-solving method

7.5.1.1. Work purpose: assessment of the facility strength in cases of loading specified by the Customer, as well as its modal analysis (determination of the lowest natural frequencies and shapes).

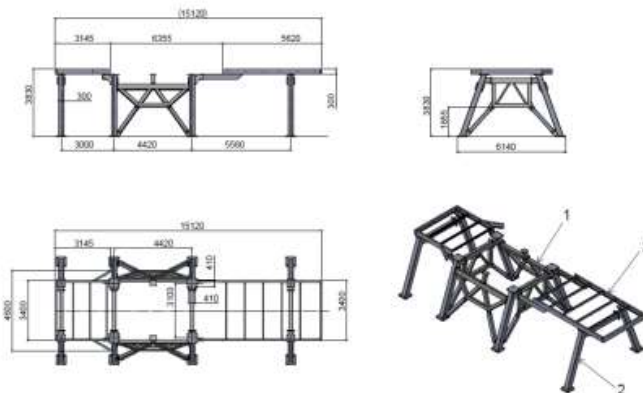
7.5.1.2. Initial information features

General view of the computer model of the load-bearing part of the facility is shown in Figure 7.5.1.

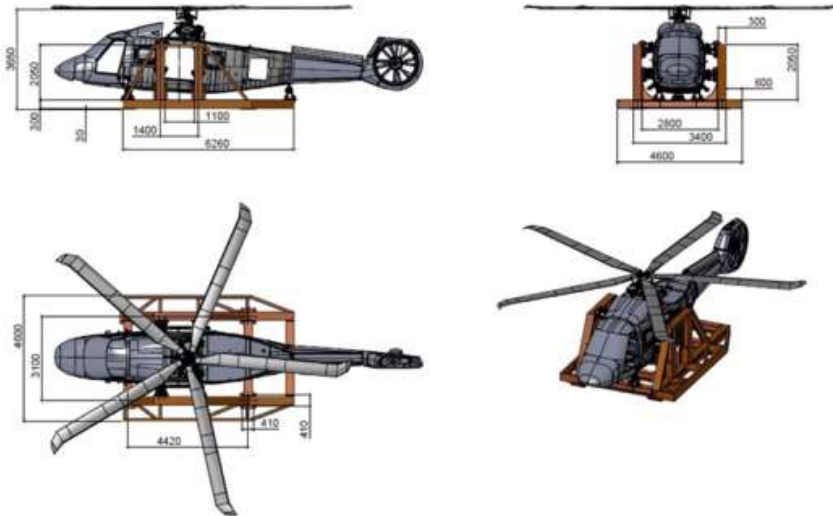
The power frame consists of a base frame and a removable module. The removable module has 11 hinge-threaded supports to fasten the helicopter.



7.5.1. Figure. General view of the computer model of the load-bearing part of the facility.



7.5.2. Figure. Base frame model



7.5.3. Figure. Removable module model with a test object

The main material of the power frame is carbon steel. For some non-bearing components, S235 mild steel was also used. The rods of the pivotally threaded supports were designed from 40X steel.

The removable module is bolted to the base frame after mounting in the helicopter fuselage module.

In turn, the helicopter fuselage is rigidly fixed to the removable module at 11 points. The main fuselage attachment points are 8 brackets specially made for the facility, fixed on two power frames:

- 4 brackets in the cab ceiling area;
- 4 brackets at the cab floor.

The indicated brackets are attached to the module through the universal pivotally threaded assemblies fixed on the module power elements (Figure 7.5.4).

Additional fuselage attachment points are the front and rear landing gear assemblies. Fastening is carried out through the nodes identical to the main ones.

Fuselage attachment points are shown in Figure 7.5.5.

An example of anchoring in the tail support area is shown in Figure 7.5.6.

General view of the model with the test object is shown in Figure 7.5.7.

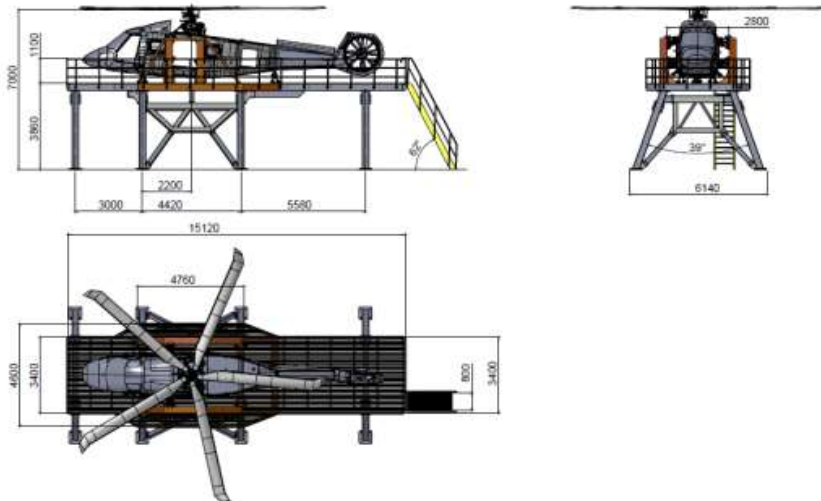
Fuselage mounting in a removable module is shown in Figure 7.5.8.

The power frame helicopter is shown in Figure 7.5.9.

The facility base frame rests on the inboard foundation. It is fixed with anchor bolts.



7.5.6. Figure. Photo of fixation in the tail support area



7.5.7. Figure. General model view with the test object



7.5.8. Figure. Fuselage assembly in a removable module



7.5.9. Figure. Helicopter on a power frame



7.5.10. Figure. Facility remote control

7.5.1.3. Problem solving method

Theoretically, the object fixing on the facility is statically indeterminate with a degree of static indeterminacy of 21. This means that a completely adequate solution to the problem of strength and stiffness can be obtained only with the presence of:

- A) The corresponding object model, adapted to solve the problem of analyzing the stress-strain state;
- B) Dynamic feature of the system.

On the other hand, the "facility - object" system is very complex. For example, each of the pivotally threaded supports is a very complex structure, so the stress analysis of the entire facility together with the object requires very significant resources. Therefore, the entire system should be simplified as much as possible.

Given these circumstances, the following problem-solving plan was adopted:

- Splitting the system into two simpler ones:
 - 1) main facility structure without supports and
 - 2) supports;
- Calculation of the main facility structure for strength and rigidity without object simulator;
- Calculated determination of the elastic compliance of each support;
- Determination of loads on supports and assessment of their strength;
- Creation of an object simulator (OS);
- Strength assessment of the main facility structure with OS when it is fixed on the facility with the system of virtual springs with compliance fully corresponding to the support flexibility;
- Modal analysis of the isolated main facility structure;
- Modal analysis of the facility with OS.

7.5.2. Generalized results of strength assessment of the main facility structure without OS

It can be seen from Table 7.5.1 that the strength of the main facility structure meets the requirements in all load cases, excluding all options of case 6 – detachment of one main rotor blade. The safety factors for options 6.1-6.3 are especially low, and their value does not exceed 1. This means that the structure cannot withstand the design load. At the same time, the strength is limited by the auxiliary facility elements. The connection of the lateral reinforcement frame with the lower inclined rods should be destroyed.

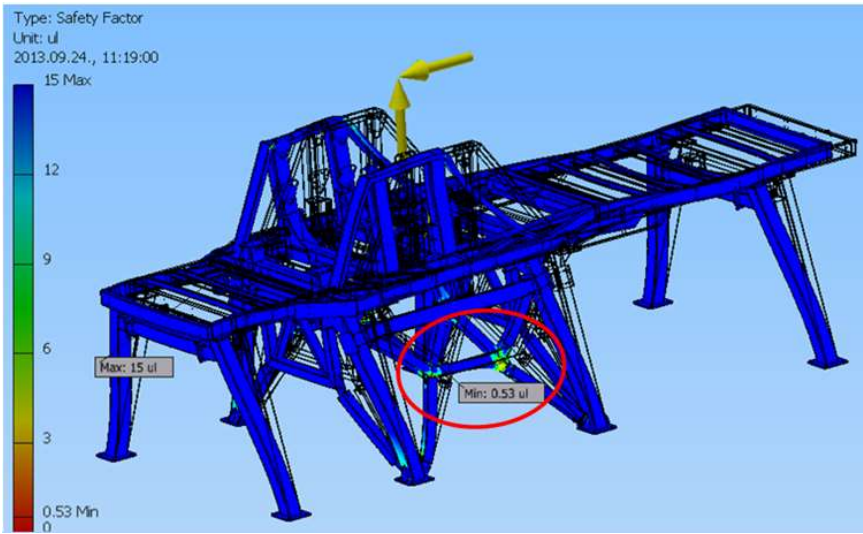
There is a comparison of two calculation options with the same load below: the vertical force of the main rotor and the horizontal force of inertia that occurs when one blade breaks off and is directed forward.

In the first option (6.1), the facility has the original configuration, and in the second (6.7), the side reinforcing frames are removed from the model, which simulates their destruction. There are Figures of the safety factor distribution according to the Mises criterion. In the first option, the maximum stresses arise in the specified area of the side reinforcing frame and they correspond to the minimum safety factor (Figure 7.5.11). In the second option, after the side reinforcing frame was removed, another place became critical - the connection of the right front column of the base frame with the right horizontal beam of the frame, and the minimum safety factor increased to 1.39 (Figure 7.5.12). This is less than required, but in this case it is possible without great difficulty to repair the weakened structure section and bring its strength to the required level.

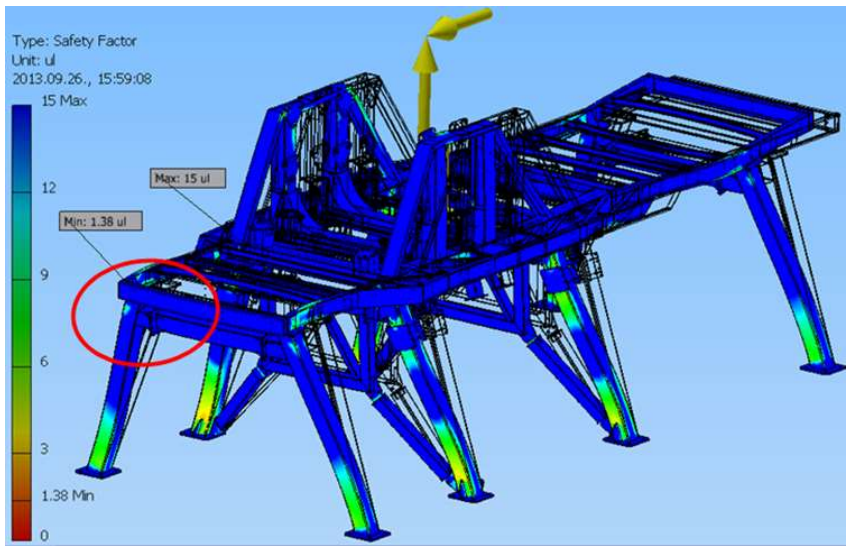
It can also be seen that the removal of the side frame leads to an increase in the stresses in the bearing elements, which, however, remain lower than the permissible ones.

Generalized results of strength calculation

Load case number	Option	Equivalent maximum von Mises stresses, MPa	Material yield strength, MPa	Calculated safety factor	Required safety factor
1	1.1	43.8	350	7.25	4
2	2.1	38.39	350	9.12	4
	2.2	37.03	350	9.45	4
	2.3	69.22	350	5.06	4
3	3.1	66.44	350	5.27	4
	3.2	67.65	350	5.17	4
	3.3	58.84	350	5.95	4
4	4.1	28.75	350	12.17	4
	4.2	27.52	350	12.72	4
5	5.1	22.42	350	15.61	4
6	6.1	662	350	0.53	2.16
	6.2	648	350	0.54	2.16
	6.3	500.9	350	0.7	2.16
	6.4	242.2	350	1.44	2.16
	6.5	248.1	350	1.41	2.16
	6.6	253	350	1.38	2.16
	6.7	251.9	350	1.39	2.16
	6.8	194.6	350	1.8	2.16
	6.9	192.4	350	1.82	2.16
7	7.1	93.61	350	3.74	2.16
	7.2	83.99	350	4.17	2.16



7.5. Figure. 11



7.5.12. Figure.

Conclusions on the strength assessment of the main facility structure without OS:

- 1) In the initial configuration, the main facility structure has the required level of strength in all standard loading cases (1-5), as well as in emergency 7 (separation of one tail rotor blade).
- 2) In an abnormal case of loading 6 (separation of one rotor blade), the facility strength in the initial configuration is insufficient and is limited by the strength of the side reinforcing frames of the base frame carrier module (loading options 6.1-6.3).
- 3) If the destruction of these facility components and their complete removal from the design model are assumed, then the facility can withstand the loads of case 6, but with safety factors less than required (load cases 6.4-6.9). In this configuration, the strength of the main structure is less than required in some areas of the removable module, as well as the front module of the base frame.
- 4) It seems that the marked critical points of the structure can be strengthened by installing (welding) additional linings, without significant changes in the basic facility structure.

7.5.3. Strength calculation of the main facility structure with installed object simulator

Object simulator

In order to completely assess the facility strength, and, mainly, its modal features, an object model was created. This model reflects the object features to some extent.

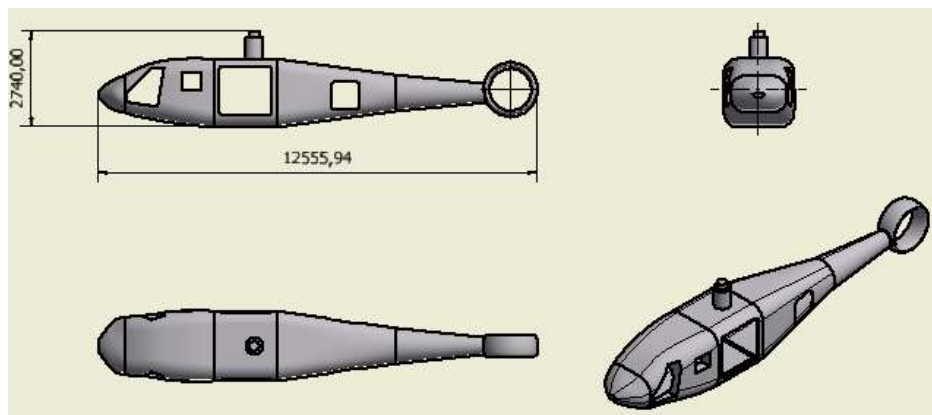
The model reproduces:

- overall dimensions (length, distance to the main rotor rotation plane), -
- approximately, its shape and some layout details (cutouts for cargo hatches, doors, windows).

Model weight is 5,800 kg. In accordance with the general ideas about the structural scheme of the object body, the shell structure thickness of the model was chosen. It is assumed that the rigidity of such a model is slightly higher than the real object rigidity, in most cases.

It was carried out a modal analysis of a loose model. The first three natural frequencies are equal, respectively: 22.08, 23.73, 32.98 Hz.

The first two vibration modes are mainly due to the stiffness of the tail rotor housing simulator, and the third is the shell shape of the body rear part.



7.5.13. Figure. Object simulator model

This model is called the object simulator and is hereinafter referred to as OS.

OS was fixed on the facility using 11 virtual springs with compliance characteristics that similar to these parameters of the pivotally threaded supports obtained in a separate section.

Provision of calculation option

There are calculation results for load case 6.4 below: Separation of one rotor blade. Vertical force 85 kN (thrust) and horizontal force of inertia (lateral 90° from right to left) 278.7 kN are applied to the gearbox shaft. It is assumed that the side reinforcement frame has been destroyed and removed from the model. There are three Figures Figure 7.5.14) in a generalized form reflecting the distribution of equivalent von Mises stresses, displacements and safety factor. This last parameter is the main one to assess strength.

In the first two Figures (7.5.14 a, b) one can see the maximum values of stresses and displacements with location indication, and in the third (7.5.14 c) - the minimum value of the safety factor.

Summarized results and conclusions with an installed object simulator.

7.5.2. Table

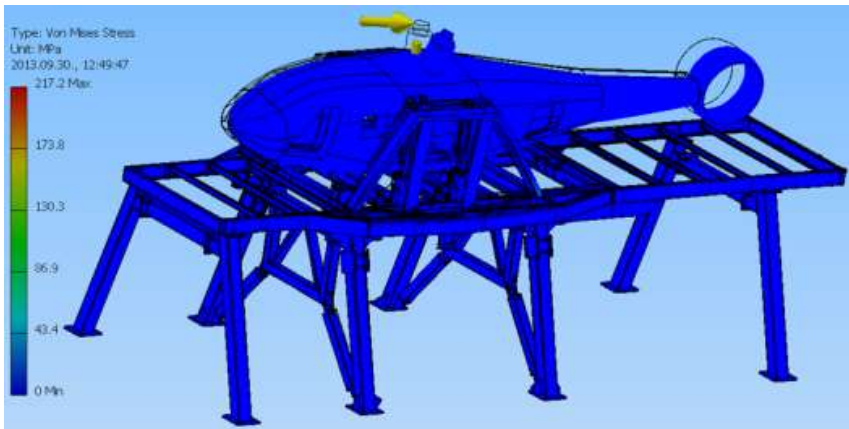
Generalized results of the facility strength calculation together with the object model

Load case number	Option	Equivalent maximum stresses according Mises, MPa	Material yield strength, MPa	Calculated safety factor	Required safety factor
6	6.4	217.2 (242.2)	350	1.61 (1.44)	2.16
	6.6	252.1 (253)	350	1.39 (1.38)	2.16
	6.7	253.6 (251.9)	350	1.38 (1.39)	2.16
	6.9	172 (192.4)	350	2.03 (1.82)	2.16

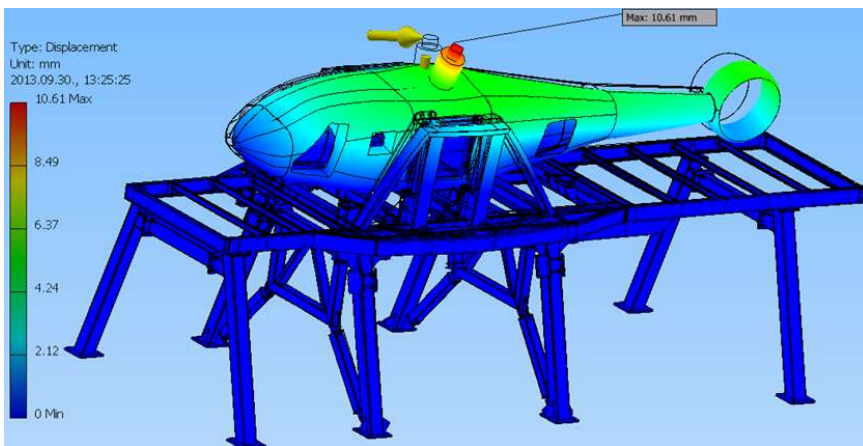
The values of the maximum von Mises stresses and safety factors obtained in the calculations of an insulated facility without object model are given in brackets.

Conclusions:

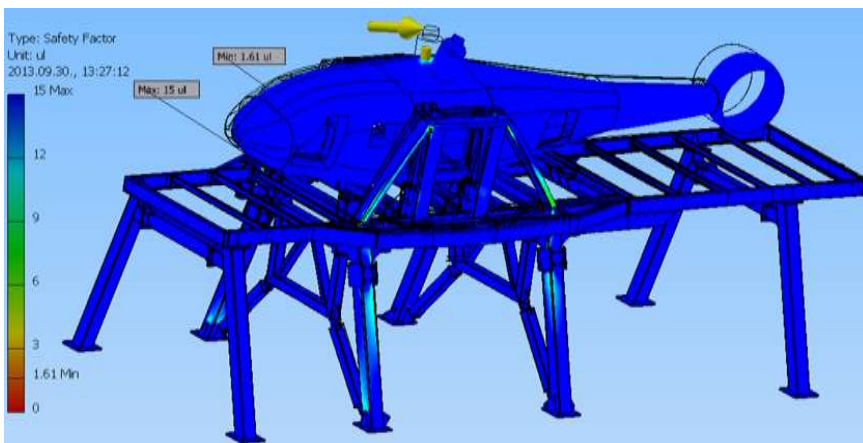
1. The maximum equivalent von Mises stresses and safety factors are of the same order as for an isolated facility without the object model. To a certain extent, this confirms the reliability of calculations.
2. Calculations confirm that the facility structure withstands the design load without destruction, but with a safety factor less than required in all options of an abnormal loading case (separation of one main rotor blade).
3. The critical areas, in which the maximum equivalent stresses act in the considered loading cases, unambiguously coincide for the two calculation models. Therefore, recommendations for possible revision of the facility structure remain unchanged.



a)



b)



c)

7.5.14. Figure

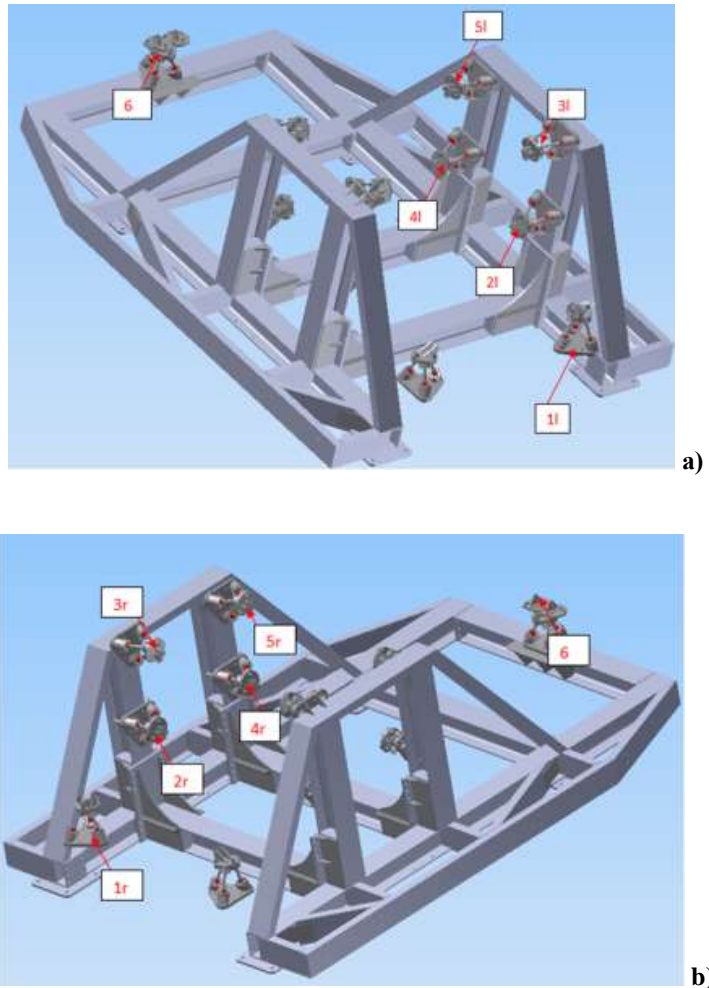
7.5.4. Analysis of loading and strength of supports

The following problem-solving plan was adopted:

- 1) determination of compliance and stresses of insulated supports.
- 2) analysis of the loading and stress state of the supports in the working position in the estimated loading design cases.

7.5.4.1. Analysis of compliance and stress of insulated supports

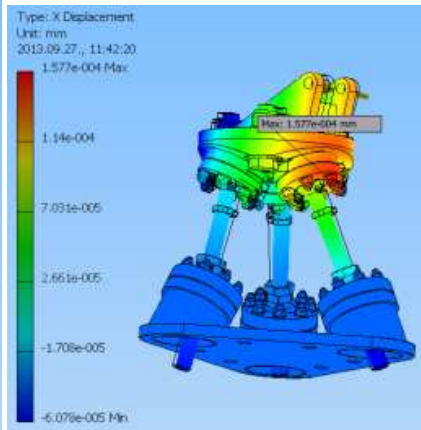
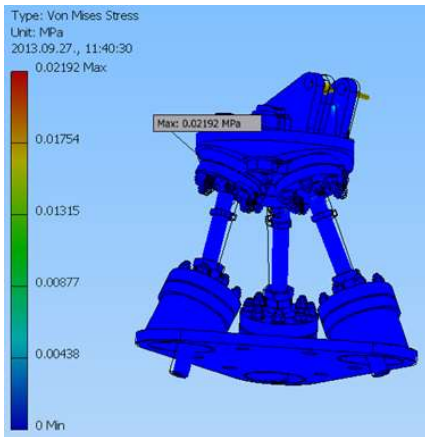
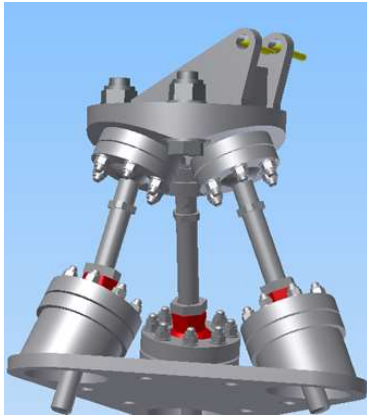
The support numbering scheme is shown in Figure 7.5.14 (a, b).



7.5.14. Figure. Support numbering scheme

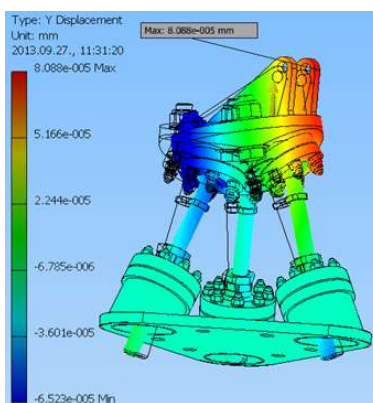
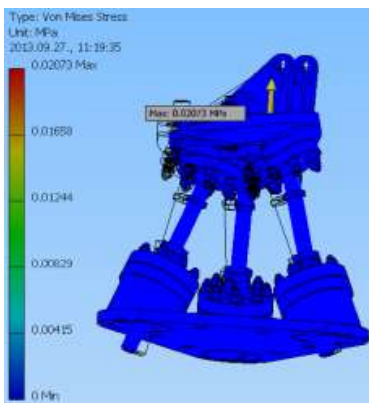
The pivotally threaded supports of the facility have a different installation configuration and different transition assemblies for connection with the object body. Therefore, an analysis of the compliance and stresses of the insulated supports is performed first. Presentation of the calculation results for support 11 (front left) is shown below.

A) A unit force (1N) is applied in the direction of Ox axis to the lug for connection with the corresponding bracket of the object. The maximum stresses in the support were obtained with the indication of the place of their occurrence and displacement in the direction of Ox axis.



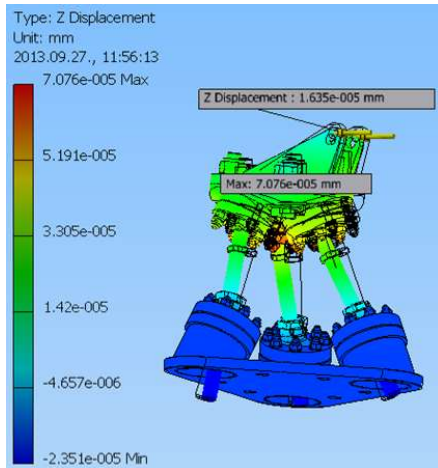
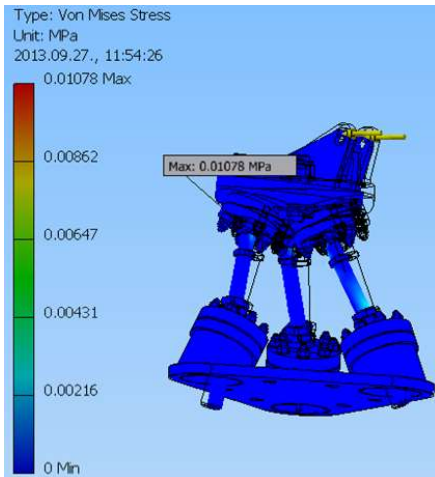
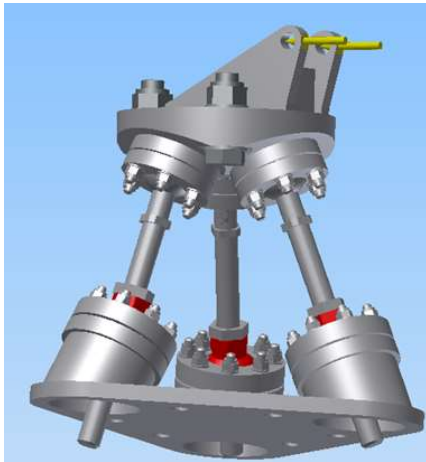
7.5.15. Figure.

B) A unit force (1N) is applied in the direction of O_y axis to the lug for connection with the corresponding bracket of the object. The maximum stresses in the support were obtained with the indication of the place of their occurrence and displacement in the direction of O_y axis.



7.5.16. Figure.

C) A unit force (1N) is applied in the direction of Oz axis to the lug for connection with the corresponding bracket of the object. The maximum stresses in the support were obtained with the indication of the place of their occurrence and displacement in the direction of Oz axis.



7.5.17. Figure.

The flexibility of removable module was also determined at the support locations. Similar calculations were performed for all other supports.

7.5.4.2. Support strength analysis

The analysis was carried out using a design model of a rigid body on 11 elastic supports with compliance that coincides with the compliance of pivotally threaded supports specified in the previous paragraph.

The calculations were performed for all design loading cases, except for case 5.

7.5.3. Table

Summary calculation results for the loading and strength of supports

Load case number	Option	Equivalent maximum von Mises stresses, MPa	Material yield strength, MPa	Calculated safety factor	Required safety factor	Critical support number
1	1.1	66.63	350	5.25	4	3l
2	2.1	87.07	350	4.02	4	3l
3	3.1	90.37	350	3.87	4	6
4	4.1	87.17	350	4.02	4	3l
	4.2	64.6	350	5.42	4	3r
5					4	
6	6.1	1,420.36	350	0.25	2.16	3r
	6.2	1,448.82	350	0.24	2.16	3r
7	7.1	691.5	350	0.51	2.16	6
	7.2	390.79	350	0.90	2.16	

Conclusions:

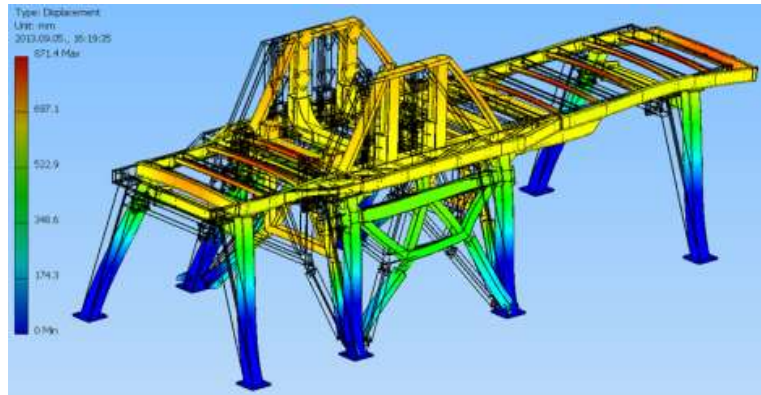
1. The design safety factor of the pivotally threaded facility supports is not lower than the load required in standard cases 1, 2, 4, and in the standard case 3 (loading by the main rotor thrust with a deviation of the thrust vector backwards), the calculated safety factor is slightly less than the required one due to the rear support overload 6.
2. In emergency loading cases 6 and 7 (separation of one main rotor blade or TR), the support strength is insufficient.

7.5.5. Modal analysis of dynamic features of the facility

7.5.5.1. Modal analysis of an isolated main facility structure

The frequencies and shapes of 10 natural vibration modes are obtained. It is given the first basic mode of the isolated facility for illustration (Figure 7.5.18):

frequency 15.47 Hz, intensive longitudinal movements of the upper part of the facility.



7.5.18. Figure.

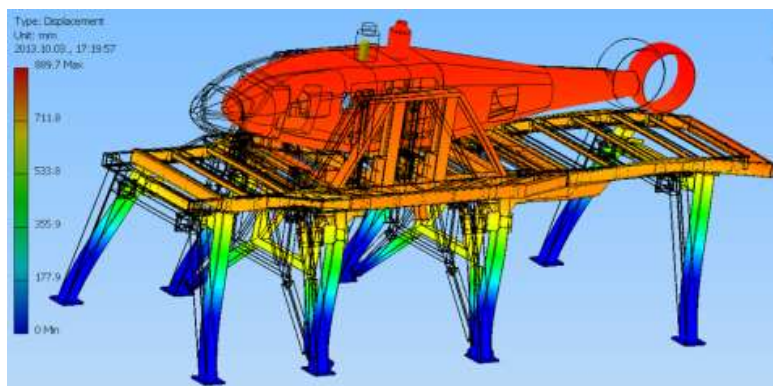
It can be concluded from the general analysis that the bearing part of the facility is intensely excited at 1, 3, and 4 frequencies. In most cases, this excitation is due to the lower rigidity of the secondary structural elements of the facility.

7.5.5.2. Modal analysis of the facility with OS

The frequencies and shapes of 10 natural vibration modes are obtained.

It is given the first main mode of the facility with OS for illustration (Figure 7.5.19).

The frequency is 7.03 Hz. Longitudinal vibrations of the OS body are similar to the rigid body. It can be seen that the displacements of all OS points are almost the same. The facility is as of the main elastic element and its deformations are significant.



7.5.19. Figure.

Conclusions:

1. From the standpoint of the dynamic strength of the facility, the most dangerous is the main (first) mode with a natural frequency of 7.03 Hz. Estimates show that taking into account the differences between OS and object, the imperfect boundary conditions and other factors that are difficult to model, the true fundamental (first) natural frequency should not differ from the obtained value by more than 10%. Apparently, this frequency may turn out to be the most significant in assessing the dynamic properties of the entire system and planning the commissioning procedure.
2. First of all, the second mode with a frequency of 14.66 Hz deserves attention of the higher modes, since it is associated with a possible intense resonance of the object tail boom. Most likely that this frequency is lower for the object, but it can be refined as a result of relatively simple experiments after the object is installed on the facility.
3. The third mode (frequency 17.74 Hz), approximately corresponding to the plane-parallel motion of the OS as a rigid body in the horizontal plane (a combination of translational movement in the lateral direction and rotation around the vertical axis) poses danger to the removable module of the facility.
4. Vibration modes associated with the excitation of the tail rotor casing (frequencies 18.43, 26.18, 30.70 Hz) have only a qualitative value for assessing possible dynamic reactions, since the differences between this part of OS and object are apparently the most significant.
5. Vibration modes (frequencies 18.41, 27.81, 32.07 Hz) demonstrate different options of the probable dynamic mutual influence of the object and the facility in the operating modes.

7.6. Receiving signals from the Facility Measurement System and their processing

In order to monitor technical condition of the facility during tests, the signals were recorded from the accelerometers installed on the power frame and the fuselage of the helicopter.

The sensors are installed in the following locations (Figure 7.6.1):

- upper part of the main gearbox, measurement was made along OX, OY, OZ axes.
- tail boom, measurement was made along OZ, OY axes;
- power frame.

Measured parameters are synchronized in time:

- rpm of the main rotor of the helicopter;
- position and movement of the helicopter controls;
- vibration (vibration acceleration in “g” units).



7.6.1. Figure. Diagram of accelerometer Installation on the facility frame

7.6.1. Type of applied accelerometers

BC 110 accelerometer with the operation principle under the piezoelectric effect (external view is shown in Figure 7.6.2).

Measured frequency range: 0.5 ... 10,000 Hz



7.6.2. Figure. External view of the BC 110 accelerometer

The accelerometers were mounted using magnetic cubes to install the AM51 accelerometers (Figure 7.6.3).



7.6.3. Figure. Magnetic cube to install accelerometers

7.6.2. Signal format received from the accelerometer

Signals from accelerometers are synchronized in time with the position of the helicopter controls:

- total blade pitch;
- longitudinal control handle;
- transverse control handle;
- tail rotor pitch.

Example of vibration signal parameters (sampling frequency 19,200 Hz) in EXEL format:

CATMAN TEST FILE

PATH=D:\CatmanWork\CatmanDataFiles

Job name=Job1

Data file with path=D:\CatmanWork\CatmanDataFiles\XXX_Job1_2015_09_22_16_20_28.bin

Data file=HC762_Job1_2015_09_22_16_20_28.bin

File comment=

Operator=

Departement=

Comment=

Default sample rate=300 Hz

Slow sample rate=5 Hz

Fast sample rate=19200 Hz

Storage mode=Fast Stream

Start mode=Manual

Start time=22.09.2015 16:20:28

Stop mode=Manual

Stop time=22.09.2015 16:20:53

catmanEasy/AP version=4.0.3.87

Numerical precision=8 Byte Float

DATAFILE=C:\Users\User\...\Ch1.XLS

7.6.3. Examples of recorded accelerometer signals from the helicopter testing

There are examples of recorded signals during testing in Figures 7.6.4-7.6.4 below.

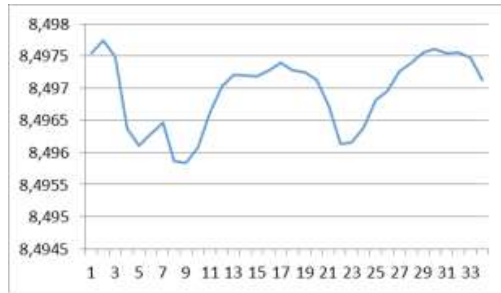
Vibration signals were recorded for all sensors at the testing start in various modes. It was made a decision on critical areas: vibration level on the main gearbox and some of the power frame sensors are considered to be control sensors. The initial signals from these sensors are designated as the "initial vibration portrait of the object".

It was made the decision: the deviation of vibration acceleration values for these sensors by an amount greater than the specified one should be considered an emergency. In this case, the tests should be stopped and the object and the facility should be examined.

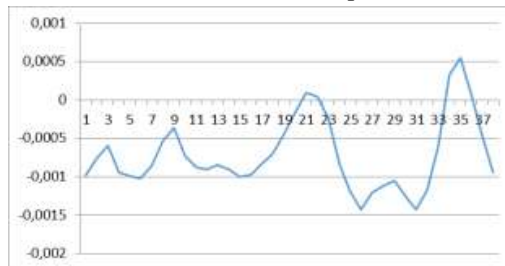
Figure 7.6.8 shows an example of the engineer's display with the current position of controls and signals from the measurement system during testing.

Figure 7.6.9 shows an example of the engineer's display with the output of signal graphs from the measurement system.

Position of the controls of the helicopter carrier system.



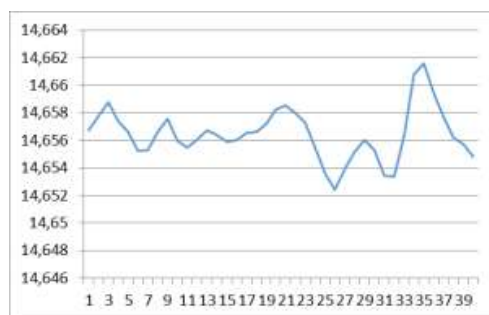
A) Position of the collective pitch handle



B) Position of the longitudinal control handle



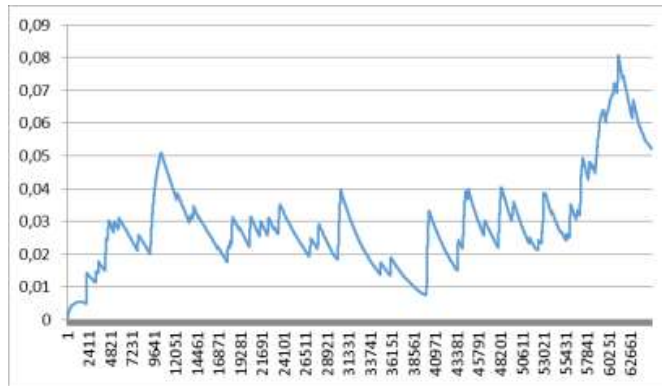
C) Position of the transverse control handle



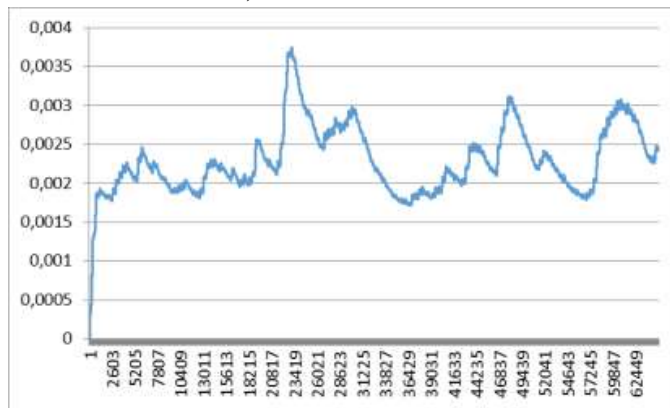
D) Tail rotor pitch

7.6.4. Figure. An example of recording the position signals of controls

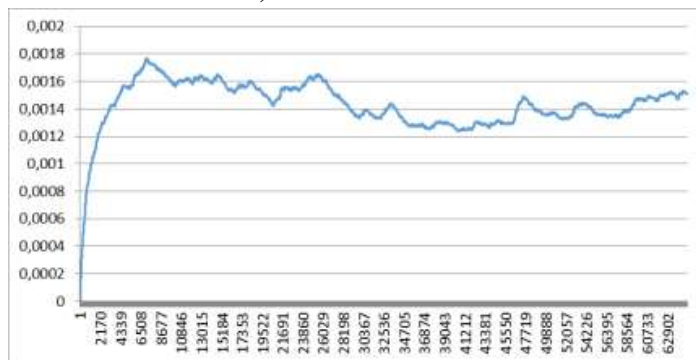
An example of signals from accelerometers (vibration acceleration in “g” units).



A) Power frame nose

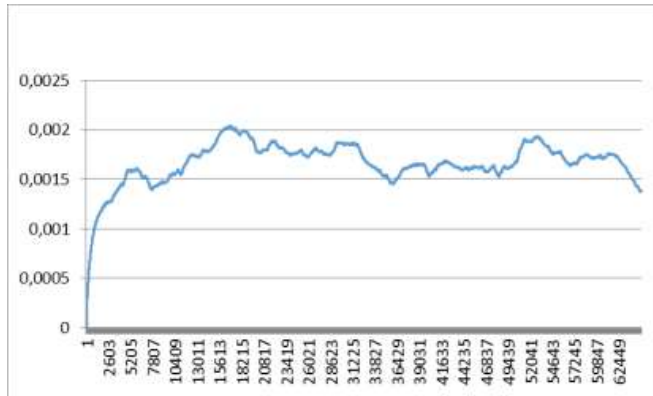


B) Power frame rear

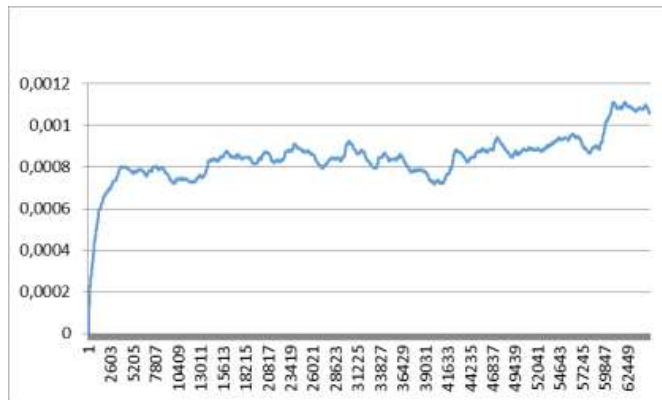


C) Power frame middle part

7.6.5. Figure. An example of recording vibration acceleration signals from sensors located on the load frame

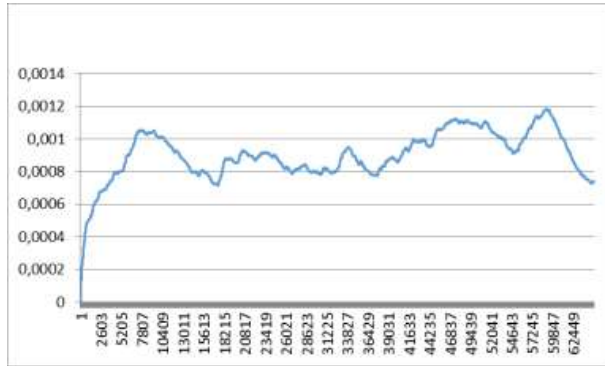


Tail boom along OZ axis

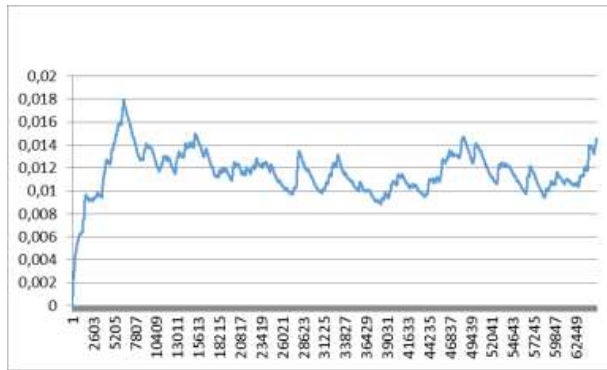


Tail boom along OY axis

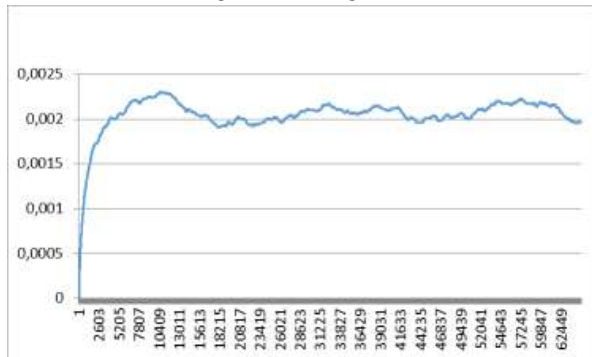
7.6.6. Figure. An example of recording vibration acceleration signals from sensors located on the tail boom



Main gearbox along OX axis

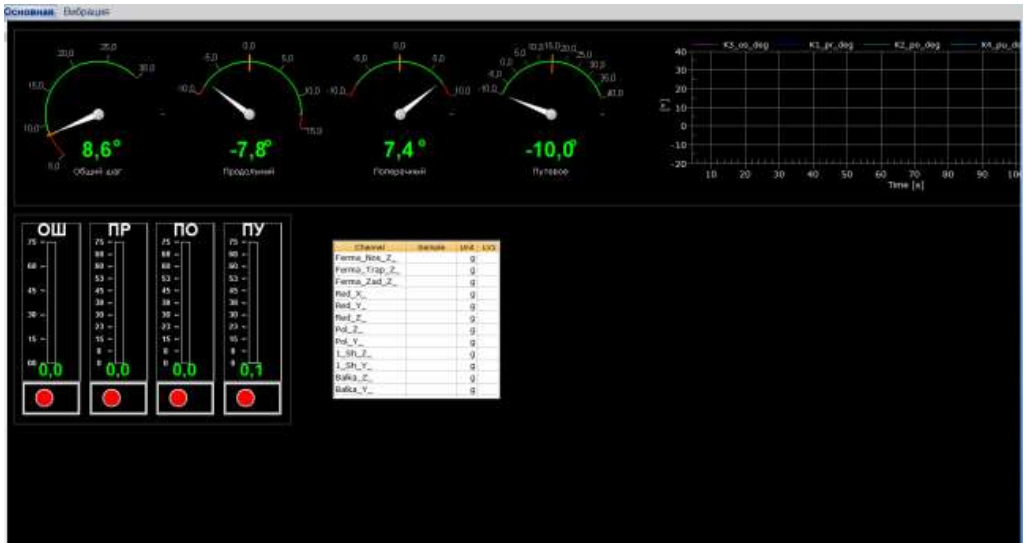


Main gearbox along OY axis

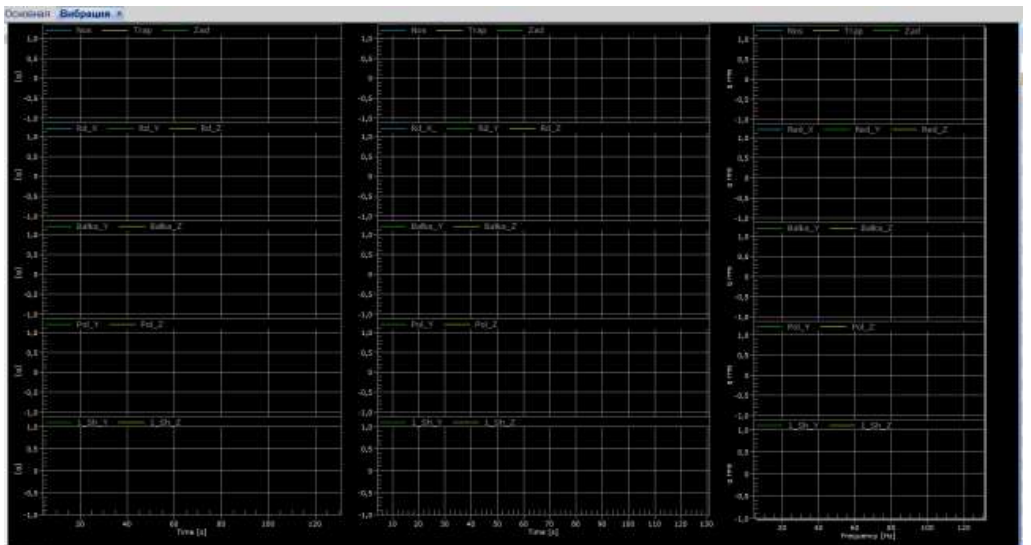


Main gearbox along OZ axis

7.6.7. Figure. An example of recording vibration acceleration signals from sensors located on the main gearbox



7.6.8. Figure. An example of the engineer's display with the current position of controls and signals from the measurement system



7.6.9. Figure. An example of the engineer's display with the output of signal graphs from the measurement system

8. Conclusions

8.1. The importance of an adequate description of the boundary conditions for the correct result is shown. Some basic regularities of the influence of boundary conditions on the dynamic properties of an elastic dynamical system are shown. A simple example shows the specific effect of elastic matching of constraints. The increase in elastic bonds reduces the natural frequencies. It can be seen that there is some critical compatibility of support for higher modes. If the match exceeds its critical value, the corresponding mode is almost insensitive to the compliance of this restriction. A critical match for a higher regime is less. In the case of the disappearance of certain restrictions, the lower vibrational modes also disappear, and their number is equal to the number of new degrees of freedom. These properties are common for an elastic system of any complexity.

8.2. A simplified model of an elastic beam is considered to evaluate the effect of the correspondence of boundary conditions to the main dynamic characteristics.

8.3. A more complex simulation of the elastic attachment of the body was made using the example of tail boom compartments of Mi-8 and Ka-62 helicopters.

8.4. The general problems of using the vibration non-destructive testing method for monitoring the state of a structure (SHM) in a full-scale testing of aircraft components are considered. It is shown that the solution can be found if the application of the method is limited to certain conditions. The main limitation is the limitation of the size of the controlled area of the structure. Those, the SHM system must be local. The second condition shown in this work, the SHM system should be objectively oriented. This means that the type of damage, its location, the size to be determined, must be known.

It is shown that with certain limitations a local monitoring system (SHM) based on vibration can be developed and practical is used in operation.

8.5. Within the framework of the Operational Modal Analysis (OMA) approach, a solution has been developed to detect a small structural damage. In this case, the excitation of the main structure occurs at a relatively low frequency. This frequency is close to the first natural frequency of the entire structure and is much smaller than the first "local" natural frequency of the observed band.

8.6. An approach to the development of a prospective damage index (diagnostic feature) for detecting small lesions in a large structural component is formulated. In this case, one or more sensors should be placed in a controlled area for measuring the signal. The base level of the dynamic response of an intact structure in the accepted excitation mode determines an intact controlled structure. Comparison of the current measurement of the output signal with the baseline gives an index for evaluating the state of the structure.

8.7. Statistical analysis of CCD (correlation coefficient deviation) index for the structural damage detection by vibration-based method was performed. Statistic data set was collected in a full-scale

test of a large aircraft component. After special pre-processing the most informative narrow frequency band was selected for obtaining the statistic set of CCD between the frequency response functions of intact and pseudo-damaged states of a structure. The two-sample Kolmogorov-Smirnov hypothesis test was used for estimation of a pseudo-damage effect. The stable response of CCD index to a small damage in large-size structure was demonstrated.

8.8. The results of the research show that the problem of detecting small lesions in a large-scale structure with low-frequency excitation with an accuracy of admissible in operation can be successfully solved.

8.9. The paper shows an example of developing a test bench with an analysis of its dynamic strength and elements of built-in continuous monitoring of the technical state of the bench and the test object. The practical application of the results of the analysis of the vibration signal is shown on the example of a stand for testing the main gearbox and transmission of a helicopter. This made it possible to reliably monitor the state of the system: helicopter-power frame.

9. Bibliography

- [1] J. L. Crassidis and John L. Junkins, *Optimal Estimation of Dynamic Systems. Applied Mathematics and Nonlinear Science Series*. Chapman and Hall/CRC, Boca Raton, FL, 2004.
- [2] J. P. Conte, X. He, B. Moaveni, S. F. Masri, J. P. Caffrey, M. Wahbeh, F. Tasbihgoo, D. H. Whang, and A. Elgamal, “Dynamic Testing of Alfred Zampa Memorial Bridge,” *Journal of Structural Engineering*, ASCE, vol. 134, issue 6, pp. 871–1066, 2008. [https://doi.org/10.1061/\(asce\)0733-9445\(2008\)134:6\(1006\)](https://doi.org/10.1061/(asce)0733-9445(2008)134:6(1006))
- [3] B. Peeters, J. Maeck, and G. De Roeck, “Vibration-based damage detection in civil engineering: excitation sources and temperature effects,” *Smart materials and Structures*, vol. 10, pp. 518–527, 2001. <https://doi.org/10.1088/0964-1726/10/3/314>
- [4] P. J. Schubel, R. J. Crossley, E. K. G. Boateng, and J. R. Hutchinson, “Review of structural health and cure monitoring techniques for large wind turbine blades,” *Renewable Energy*, vol. 51, pp. 113–123, 2013. <https://doi.org/10.1016/j.renene.2012.08.072>
- [5] K. He and W. D. Zhu, “Detecting Loosening of Bolted Connections in a Pipeline Using Changes in Natural Frequencies,” *ASME J. Vib. Acoust.*, vol. 136, issue 3, pp. 034503, 2014. <https://doi.org/10.1115/1.4026973>
- [6] H. Sohn, C. Farrar, N. Hunter, and K. Worden, “A Review of Structural Health Monitoring Literature: 1996–2001,” Los Alamos National Laboratory report, (LA-13976-MS), 2003.
- [7] E. P. Carden and P. Fanning, “Vibration based condition monitoring: A review,” *Structural Health Monitoring*, vol. 3, pp. 355–377, 2004. <https://doi.org/10.1177/1475921704047500>
- [8] C. R. Farrar, S. W. Doebling, and D. A. Nix, “Vibration-based structural damage identification,” *Philosophical Transactions of the Royal Society A: Mathematical, Physical and Engineering Sciences*, vol. 359, issue 1778, pp. 131–149, 2001.
- [9] M. N. Rezai, J. E. Bernard, and J. M. Starkey, “Empirical modal analysis,” *The Shock and Vibration Digest*, vol. 15, 1983.
- [10] D. J. Ewins, *Modal Testing: Theory, Practice and Application*. Baldock: Research Studies Press, UK, 2003.
- [11] M. W. Halling, I. Muhammad, and K. C. Womack, “Dynamic testing for condition assessment of bridge bents,” *Journal of Structural Engineering, ASCE*, vol. 127, issue 2, pp. 161–167, 2001. [https://doi.org/10.1061/\(ASCE\)0733-9445\(2001\)127:2\(161\)](https://doi.org/10.1061/(ASCE)0733-9445(2001)127:2(161))
- [12] J. M. W. Brownjohn, P. Moyo, P. Omenzetter, and Y. Lu, “Assessment of highway bridge upgrading by dynamic testing and finite- element model updating,” *Journal of Bridge Engineering, ASCE*, vol. 8, issue 3, pp. 162–172, 2003. [https://doi.org/10.1061/\(ASCE\)1084-0702\(2003\)8:3\(162\)](https://doi.org/10.1061/(ASCE)1084-0702(2003)8:3(162))
- [13] M. M. Abdel Wahab and G. De Roeck, “Dynamic testing of prestressed concrete bridges and numerical verification,” *Journal of Bridge Engineering, ASCE*, vol. 3, issue 4, pp. 159–169, 1998. [https://doi.org/10.1061/\(ASCE\)1084-0702\(1998\)3:4\(159\)](https://doi.org/10.1061/(ASCE)1084-0702(1998)3:4(159))
- [14] E. Reynders, “System identification methods for (operational) modal analysis: review and comparison,” *Archives of Computational Methods in Engineering*, vol. 19, pp. 51–124, 2012. <https://doi.org/10.1007/s11831-012-9069-x>
- [15] D. E. Adams, *Health Monitoring of Structural Materials and Components: Methods with Application*. Chichester: John Wiley & Sons Ltd., 2007. <https://doi.org/10.1002/9780470511589>
- [16] V. Giurgiutiu, *Structural Health Monitoring with Piezoelectric Wafer Active Sensors*. Amsterdam & Boston: Elsevier Academic Press, 2008.
- [17] G. C. Goodwin and R. L. Payne, *Dynamic System Identification: Experiment Design and Data Analysis*. Academic Press, 1977

- [18] S. A. Billings, *Nonlinear System Identification: NARMAX Methods in the Time, Frequency, and Spatio-Temporal Domains*. Wiley, 2013. <https://doi.org/10.1002/9781118535561>
- [19] T. P. Gialamas, D. A. Manolas, and D. T. Tsahalis, "Predicting the Dynamic Behaviour of a Coupled Structure Using Frequency-Response Functions," *Journal of Aircraft*, vol. 39, issue 1, pp. 109–113, 2002. <https://doi.org/10.2514/2.2902>
- [20] P. Van Loon, *Modal Parameters of Mechanical Structures*, Ph.D. Dissertation, Dept. of Mechanical Engineering, Katholieke Universiteit Leuven, Leuven, Belgium, 1974.
- [21] G. W. Housner, L. A. Bergman, T. K. Caughey, A. G. Chassiakos, R. O. Claus, S. F. Masri, R. E. Skelton, T. T. Soong, B. F. Spencer, J. T. P. Yao, "Structural control: past, present, and future," *Journal of Engineering Mechanics*, vol. 123, pp. 897–971, 1997. [https://doi.org/10.1061/\(ASCE\)0733-9399\(1997\)123:9\(897\)](https://doi.org/10.1061/(ASCE)0733-9399(1997)123:9(897))
- [22] J. T. Xing, Y. P. Xiong, and W. G. Price, "A generalized mathematical model and analysis for integrated multi-channel vibration structure–control interaction systems," *Journal of Sound and Vibration*, vol. 320, pp. 584–616, 2009. <https://doi.org/10.1016/j.jsv.2008.08.009>
- [23] G. Dimitriadis, "Bifurcation Analysis of Aircraft with Structural Nonlinearity and Free play Using Numerical Continuation," *Journal of Aircraft*, vol. 45, issue 3, pp. 893–905, 2008. <https://doi.org/10.2514/1.28759>
- [24] Hua-Peng Chen, "Nonlinear Perturbation Theory for Structural Dynamic Systems," *AIAA Journal*, vol. 43, issue 11, pp. 2412–2421, 2005. <https://doi.org/10.2514/1.15207>
- [25] Y. G. Panovko and I. I. Gubanov, *Stability and Oscillations of Elastic Systems: Paradoxes, Fallacies, and New Concepts*. Translated by Chas. V. Larrick, New York: Consultants Bureau, 1965.
- [26] S. Kuzņecovs, Ē. Ozoliņš, I. Ozoliņš, I. Pavelko, and V. Pavelko, "Dynamic Properties and Fatigue Failure of Aircraft Component," in *Engineering against Fracture: Proceedings of the 1st Conference*, Greece, Patras, 28–30 May, 2008. Amsterdam: Springer Science, 2009, pp. 105–114. ISBN 9781402094019. e-ISBN 9781402094026. https://doi.org/10.1007/978-1-4020-9402-6_9
- [27] Doebling S W, Farrar C R, and Prime M B 1998 *Shock Vib Dig* **30(2)** 91
- [28] Jun Lia, and Hong Hao 2016 *Structural Monitoring and Maintenance* **3(1)** 33
- [29] Pandey A K, Biswas M, and Samman M M 1991 *J Sound Vib* **145(2)** 321
- [30] Ratcliffe C P 2000 *ASME J Vib Acoust* **122(3)** 324
- [31] Pavelko V, and Shakhmansky G 1971 *Trans of Riga Institute of Civil Aviation* **191** 18
- [32] Pavelko I, and Pavelko V 1997 *Proc Int Conf. (Pranesimus medziaga Transporto priemones – 97) Kaunas, Lithuania. Technology* 237
- [33] Ebrahimi A, Behzad M, and Meghdari A 2010 *Int J Mechl Sci* **52** 904
- [34] Swapnil Dokhe, and Shailesh Pimpale 2015 *Int J Res Aer Mech Eng* **3(8)** 24
- [35] Liang RY, Hu J L, and Choy F 1992 *J Eng Mech-ASCE* **118** 384
- [36] Kasper D G , Swanson D C, and Reichard K M 2008 *Journal of Sound and Vibration* **312** 1
- [37] Pfeiffer H, Pitropakis I, and Wevers M. 2010 *Proc 10th European Conference on Non-Destructive Testing Moscow* www.ndt.net
- [38] Prakash Rajendrana, and Sivakumar M Srinivasan 2015 *Structural Engineering and Mechanics* 54(4) 711
- [39] Pitropakis I, Pfeiffer H, and Wevers M. 2012 *Sensors and Actuators A Physical* **176** 57
- [40] Mays L W, and Tung Y K 1992 *Engineering and Management* McGraw-Hill, NY USA
- [41] Naidu A S K, Bhalla S, and Soh C K 2002 *Proc SPIE* **4935** 473
- [42] Giurgiutiu V, Zagrai A, and Bao J J 2002 *Int J Structural Health Monitoring* **1** 41
- [43] Annamdas V G M, and Soh Ch K 2010 *J Intel Mat Syst Struct* 21 41
- [44] А.И.Макаревский, В.М.Чижов. Основы прочности и аэроупругости летательных аппаратов.- Москва: Машиностроение, 1982.-238 с.

- [45] Airworthiness of Aircraft. Annex 8 to the Convention on International Civil Aviation
- [46] Airworthiness Manual: Volume I--Organization and Procedures by International Civil Aviation Organization (Creator), 412 pages. Published January 1st 2001 by International Civil Aviation Organization
- [47] Filippo de Florio. Airworthiness: An Introduction to Aircraft Certification-- Elsevier, First edition 2006/-247 pages
- [48] Airbus A380 Wing-Fuselage Testing. <https://www.youtube.com/watch?v=z19m9LZOOZY>
- [49] A-380. The wings on this Airbus flex way more than they should. https://www.youtube.com/watch?v=-LTYRTKV_A
- [50] Boeing 787 Wing Testing. <https://www.youtube.com/watch?v=meEG7VwjTew>
- [51] Pushing the A350 XWB to the brink. https://www.youtube.com/watch?v=B74_w3Ar9nI
- [52] Boeing 787 conducts fatigue testing. <https://www.youtube.com/watch?v=TH9k9fWaFrs>
- [53] Original Wing test JS1 Revelation. <https://www.youtube.com/watch?v=M6VBqsrD4FE>
- [54] Of Struggle and Flight/ The History of Latvian Aviation by , Kārlis Irbitis, Rīga, RTU Press, 2006.- (117) 211 p.
- [55] Riga, SIA “Aviatest LTD”, “Bench for testing the Ka-62 helicopter for static strength”, 2016 – (17) 44 p.
- [56] "Full-size stand of the Mi-26 helicopter"
- [57] “Stand for fatigue testing of the Mi-38 helicopter fuselage” 2015, Riga, SIA “Aviatest LTD”
- [58] “Bench for fatigue testing of the fenestron of the Ka-62 helicopter” Riga, SIA “Aviatest LTD”, 97 p.
- [59] Riga, SIA “Aviatest LTD”, 2017, “Sample testing”
- [60] Riga, SIA “Aviatest LTD”, Техническая справка №АТ-ТЛ.01-15/16г, 2016 – 12 p.
- [61] Riga, SIA “Aviatest LTD”, 2014, “Elevator destruction”
- [62] “On the Dynamic Response Prediction at the Full-Scale Test of Aircraft Component”, Transport and Aerospace Engineering, 2017, Vitaly Pavelko , Alexander Nevsky <https://tae-journals.rtu.lv/article/view/tae-2017-0003>
- [63] “Vibration-Based Detection of Small Damage in the Aircraft Large Component”, Матеріали XIII міжнародної науково-технічної конференції “АВІА-2017”, page 17.63-17.68, 2017, Vitaly Pavelko, Sergei Kuznetsov , Alexander Nevsky , Mark Marinbach <http://avia.nau.edu.ua/indexallua.php>
- [64] “Vibration-Based Structural Health Monitoring of the Aircraft Large Component”, IOP Conference Series: Materials Science and Engineering, 2017, Vitaly Pavelko , Sergey Kuznetsov, Alexander Nevsky , Mark Marinbach <https://iopscience.iop.org/article/10.1088/1757-899X/251/1/012093>
- [65] “Statistical Estimation of Perspective Damage Index for Vibration-Based Structural Health Monitoring”, Journal of Physics: Conference Series, 2019, Vitaly Pavelko , Alexander Nevsky <https://iopscience.iop.org/article/10.1088/1742-6596/1172/1/012036>
- [66] "Full-size stand of the Ka-62 helicopter", 2019, SIA “Aviatest LTD”
- [67] "Bench for testing the fatigue strength of the tail boom of the helicopter Ka-62", 2018, SIA “Aviatest LTD”
- [68] Health and Usage Monitoring System (HUMS) <https://www.skybrary.aero/articles/health-and-usage-monitoring-system-hums>



Aleksandrs Nevskis was born in 1959 in Vitebsk, Belarus. He graduated from Riga Civil Aviation University in 1983. In 1983–1993, he was a researcher of the State Research Institute of Civil Aviation Riga branch. From 1993 to 2011, he was the Director of Rinal Plus Ltd. and from 2011 to 2022, a project manager in Aviatest Ltd. His research interests are in the areas of dynamic and strength analysis of airframe constructions, dynamical characteristics prognostication during the airframe construction testing, and mathematical simulation.